48 h of stimulation with 40 ng/ml PMA and 10^{-5} M ionomycin. We used anti–human IL-17A and anti–human IL-22 Duoset kits (R&D Systems) and the anti–human IL-17F ELISA Ready-SET-GO! set (eBioscience).

Statistical analysis. We assessed differences between controls, MSMD patients bearing loss-of-function *STAT1* alleles, and CMCD patients bearing gain-of-function *STAT1* alleles in terms of the percentages of IL-17A– and IL-22–producing T cells, as assessed by flow cytometry, and in terms of the amounts of IL-17A, IL-17F, and IL-22 produced in various stimulation conditions, as assessed by ELISA. We used the nonparametric Wilcoxon test, as implemented in the PROC NPAR1WAY of the SAS software version 9.1 (SAS Institute). For all analyses, $P < 0.05$ was considered statistically significant.

Online supplemental material

Fig. S1 shows that STAT1-CMCD mutants are gain-of-function alleles by loss of nuclear dephosphorylation. Fig. S2 is a schematic representation of the cytokines and transcription factors directing the development of naive CD4 cells into IL-17–producing T cells. Fig. S3 shows the normal response of CMCD patient cells to IFN-α in terms of ISGF3 activation, to IFN-γ in terms of STAT1 nuclear translocation; and to IL-23 and IL-22 in terms of pSTAT3. Fig. S4 shows impaired in vitro differntiation of IL-17– and Il-22–producing T cell blasts in patients with CMCD and gain-of-function SATA1 mustations. Table S1 shows novel coding heterozygous variants found by whole-exome sequencing in the 6 different patients. Table S2 shows novel coding heterozygous variants found by whole-exome sequencing within genes shared by more than one patient. Table S3 lists conservation and predictions on the function of the mutant STAT1 alleles associated with CMCD. Table S4 lists the STAT1 GOF mutation created, and the pair of primers used. Online supplemental material is available at http://www.jem.org/cgi/content/full/jem.20110958/DC1.

We thank the members of the laboratory for helpful discussions; Yelena Nemiroskaya, Eric Anderson, Martine Courat, and Michele N'Guyen for secretarial assistance; and Tony Leclerc and Tiffany Nivare for technical assistance. We also thank Alekszandra Barsony, Dmitriy Samarin, Fedir Lapiy, Maxim Vodyanik, Marcela Moncada Velez, Bertrand Boisson, and Astrid Research, Inc.

This work was supported by grants from Institut National de la Santé et de la Recherche Médicale, University Paris Descartes, the Rockefeller University, the Rockefeller University CTSA grant number 5UL1RR024143-04, the St. Giles Foundation, and the Candidoser Association awarded to Jean-Laurent Casanova. Janine Reichenbach was supported by the Gebert Rüf Stiftung, program "Rare Diseases – New Approaches"; Ellen Renner by the DFG RE2799/3-1 and a Fritz-Thyssen research foundation grant (Az. 10.07.1.159). Support was also provided by TÁMOP 4.2.1./B-09/1/KONV-2010-0007 and TÁMOP 4.2.2-08/1-2008-0015 grants to László Maródi and LMU Munich FöFoLe grant #680/658. Sophie Cypowyj was supported by the AXA Research Fund, and Xiaofei Kong by the Choh-Hao Li Memorial Fund Scholar award and the Shanghai Educational Development Foundation. We have all the approvals and authorizations required for this study (Necker IRB, Paris, 1995 and Rockefeller IRB, New York, 2008).

The authors state no conflict of interest.

Submitted: 11 May 2011
Accepted: 22 June 2011

REFERENCES

Adzhubei, I.A., S. Schmidt, L. Peshkin, V.E. Ramensky, A. Gerasimova, P. Bork, A.S. Kondrashov, and S.R. Sunyaev. 2010. A method and server for predicting damaging missense mutations. *Nat. Methods.* 7:248–249. doi:10.1038/nmeth0410-248

Alcaïs, A., L. Abel, and J.L. Casanova. 2009. Human genetics of infectious diseases: between proof of principle and paradigm. *J. Clin. Invest.* 119:2506–2514. doi:10.1172/JCI38111

Alcaïs, A., L. Quintana-Murci, D.S. Thaler, E. Schurr, L. Abel, and J.L. Casanova. 2010. Life-threatening infectious diseases of childhood: single-gene inborn errors of immunity? *Ann. N.Y.Acad. Sci.* 1214:18–33. doi:10.1111/j.1749-6632.2010.05834.x

Amadi-Obi, A., C.R. Yu, X. Liu, R.M. Mahdi, G.L. Clarke, R.B. Nussenblatt, I. Gery, Y.S. Lee, and C.E. Egwuagu. 2007. TH17 cells contribute to uveitis and scleritis and are expanded by IL-2 and inhibited by IL-27/STAT1. *Nat. Med.* 13:711–718. doi:10.1038/nm1585

Atkinson, T.P., A.A. Schäffer, B. Grimbacher, H.W. Schroeder Jr., C. Woellner, C.S. Zerbe, and J.M. Puck. 2001. An immune defect causing dominant chronic mucocutaneous candidiasis and thyroid disease maps to chromosome 2p in a single family. *Am. J. Hum. Genet.* 69:791–803. doi:10.1086/323611

Averbuch, D., A. Chapgier, S. Boisson-Dupuis, J.L. Casanova, and D. Engelhard. 2011. The clinical spectrum of patients with deficiency of Signal Transducer and Activator of Transcription-1. *Pediatr. Infect. Dis. J.* 30:352–355.

Batten, M., J. Li, S. Yi, N.M. Kljavin, D.M. Danilenko, S. Lucas, J. Lee, F.J. de Sauvage, and N. Ghilardi. 2006. Interleukin 27 limits autoimmune encephalomyelitis by suppressing the development of interleukin 17-producing T cells. *Nat. Immunol.* 7:929–936. doi:10.1038/ni1375

Bentur, L., E. Nisbet-Brown, H. Levison, and C.M. Roifman. 1991. Lung disease associated with IgG subclass deficiency in chronic mucocutaneous candidiasis. *J. Pediatr.* 118:82–86. doi:10.1016/S0022-3476(05)81852-9

Bolze, A., M. Byun, D. McDonald, N.V. Morgan, A. Abhyankar, L. Premkumar, A. Puel, C.M. Bacon, F. Rieux-Laucat, K. Pang, et al. 2010. Whole-exome-sequencing-based discovery of human FADD deficiency. *Am. J. Hum. Genet.* 87:873–881. doi:10.1016/j.ajhg.2010.10.028

Braunstein, J., S. Brutsaert, R. Olson, and C. Schindler. 2003. STATs dimerize in the absence of phosphorylation. *J. Biol. Chem.* 278:34133–34140. doi:10.1074/jbc.M304531200

Byun, M., A. Abhyankar, V. Lelarge, S. Plancoulaine, A. Palanduz, L. Telhan, B. Boisson, C. Picard, S. Dewell, C. Zhao, et al. 2010. Whole-exome sequencing-based discovery of STIM1 deficiency in a child with fatal classic Kaposi sarcoma. *J. Exp. Med.* 207:2307–2312. doi:10.1084/jem.20101597

Casanova, J.L., and L. Abel. 2005. Inborn errors of immunity to infection: the rule rather than the exception. *J. Exp. Med.* 202:197–201. doi:10.1084/jem.20050854

Casanova, J.L., and L. Abel. 2007. Primary immunodeficiencies: a field in its infancy. *Science.* 317:617–619. doi:10.1126/science.1142963

Chapgier, A., S. Boisson-Dupuis, E. Jouanguy, G. Vogt, J. Feinberg, A. Prochnicka-Chalufour, A. Casrouge, K. Yang, C. Soudais, C. Fieschi, et al. 2006a. Novel STAT1 alleles in otherwise healthy patients with mycobacterial disease. *PLoS Genet.* 2:e131. doi:10.1371/journal.pgen.0020131

Chapgier, A., R.F. Wynn, E. Jouanguy, O. Filipe-Santos, S. Zhang, J. Feinberg, K. Hawkins, J.L. Casanova, and P.D. Arkwright. 2006b. Human complete Stat-1 deficiency is associated with defective type I and II IFN responses in vitro but immunity to some low virulence viruses in vivo. *J. Immunol.* 176:5078–5083.

Chapgier, A., X.F. Kong, S. Boisson-Dupuis, E. Jouanguy, D. Averbuch, J. Feinberg, S.Y. Zhang, J. Bustamante, G. Vogt, J. Lejeune, et al. 2009. A partial form of recessive STAT1 deficiency in humans. *J. Clin. Invest.* 119:1502–1514. doi:10.1172/JCI37083

Chen, X., U. Vinkemeier, Y. Zhao, D. Jeruzalmi, J.E. Darnell Jr., and J. Kuriyan. 1998. Crystal structure of a tyrosine phosphorylated STAT-1 dimer bound to DNA. *Cell.* 93:827–839. doi:10.1016/S0092-8674(00)81443-9

Chen, M., G. Chen, H. Nie, X. Zhang, X. Niu, Y.C. Zang, S.M. Skinner, J.Z. Zhang, J.M. Killian, and J. Hong. 2009. Regulatory effects of IFN-beta on production of osteopontin and IL-17 by CD4+ T Cells in MS. *Eur. J. Immunol.* 39:2525–2536. doi:10.1002/eji.200838879

Crabé, S., A. Guay-Giroux, A.J. Tormo, D. Duluc, R. Lissilaa, F. Guilhot, U. Mavoungou-Bigouagou, F. Lefouili, I. Cognet, W. Ferlin, et al. 2009. The IL-27 p28 subunit binds cytokine-like factor 1 to form a cytokine regulating NK and T cell activities requiring IL-6R for signaling. *J. Immunol.* 183:7692–7702. doi:10.4049/jimmunol.0901464

de Beaucoudrey, L., A. Puel, O. Filipe-Santos, A. Cobat, P. Ghandil, M. Chrabieh, J. Feinberg, H. von Bernuth, A. Samarina, L. Jannière, et al. 2008. Mutations in STAT3 and IL12RB1 impair the development of human IL-17-producing T cells. *J. Exp. Med.* 205:1543–1550. doi:10.1084/jem.20080321

de Beaucoudrey, L., A. Samarina, J. Bustamante, A. Cobat, S. Boisson-Dupuis, J. Feinberg, S. Al-Muhsen, L. Jannière, Y. Rose, M. de Suremain, et al. 2010. Revisiting human IL-12Rβ1 deficiency: a survey of 141 patients from 30 countries. *Medicine.* 89:381–402. doi:10.1097/MD.0b013e3181fdd832

Diveu, C., M.J. McGeachy, K. Boniface, J.S. Stumhofer, M. Sathe, B. Joyce-Shaikh, Y. Chen, C.M. Tato, T.K. McClanahan, R. de Waal Malefyt, et al. 2009. IL-27 blocks RORc expression to inhibit lineage commitment of Th17 cells. *J. Immunol.* 182:5748–5756. doi:10.4049/jimmunol.0801162

Donnelly, R.P., F. Sheikh, H. Dickensheets, R. Savan, H.A. Young, and M.R. Walter. 2010. Interleukin-26: an IL-10-related cytokine produced by Th17 cells. *Cytokine Growth Factor Rev.* 21:393–401. doi:10.1016/j.cytogfr.2010.09.001

Dupuis, S., C. Dargemont, C. Fieschi, N. Thomassin, S. Rosenzweig, J. Harris, S.M. Holland, R.D. Schreiber, and J.L. Casanova. 2001. Impairment of mycobacterial but not viral immunity by a germline human STAT1 mutation. *Science.* 293:300–303. doi:10.1126/science.1061154

Dupuis, S., E. Jouanguy, S. Al-Hajjar, C. Fieschi, I.Z. Al-Mohsen, S. Al-Jumaah, K. Yang, A. Chapgier, C. Eidenschenk, P. Eid, et al. 2003. Impaired response to interferon-alpha/beta and lethal viral disease in human STAT1 deficiency. *Nat. Genet.* 33:388–391. doi:10.1038/ng1097

El-behi, M., B. Ciric, S. Yu, G.X. Zhang, D.C. Fitzgerald, and A. Rostami. 2009. Differential effect of IL-27 on developing versus committed Th17 cells. *J. Immunol.* 183:4957–4967. doi:10.4049/jimmunol.0900735

Eyerich, K., S. Foerster, S. Rombold, H.P. Seidl, H. Behrendt, H. Hofmann, J. Ring, and C. Traidl-Hoffmann. 2008. Patients with chronic mucocutaneous candidiasis exhibit reduced production of Th17-associated cytokines IL-17 and IL-22. *J. Invest. Dermatol.* 128:2640–2645. doi:10.1038/jid.2008.139

Feinberg, J., C. Fieschi, R. Doffinger, M. Feinberg, T. Leclerc, S. Boisson-Dupuis, C. Picard, J. Bustamante, A. Chapgier, O. Filipe-Santos, et al. 2004. Bacillus Calmette Guerin triggers the IL-12/IFN-gamma axis by an IRAK-4- and NEMO-dependent, non-cognate interaction between monocytes, NK, and T lymphocytes. *Eur. J. Immunol.* 34:3276–3284. doi:10.1002/eji.200425221

Feng, G., W. Gao, T.B. Strom, M. Oukka, R.S. Francis, K.J. Wood, and A. Bushell. 2008. Exogenous IFN-gamma ex vivo shapes the alloreactive T-cell repertoire by inhibition of Th17 responses and generation of functional Foxp3+ regulatory T cells. *Eur. J. Immunol.* 38:2512–2527. doi:10.1002/eji.200838411

Filipe-Santos, O., J. Bustamante, A. Chapgier, G. Vogt, L. de Beaucoudrey, J. Feinberg, E. Jouanguy, S. Boisson-Dupuis, C. Fieschi, C. Picard, and J.L. Casanova. 2006. Inborn errors of IL-12/23- and IFN-gamma-mediated immunity: molecular, cellular, and clinical features. *Semin. Immunol.* 18:347–361. doi:10.1016/j.smim.2006.07.010

Germain, M., M. Gourdeau, and J. Hébert. 1994. Case report: familial chronic mucocutaneous candidiasis complicated by deep candida infection. *Am. J. Med. Sci.* 307:282–283. doi:10.1097/00000441-199404000-00008

Glocker, E.O., A. Hennigs, M. Nabavi, A.A. Schäffer, C. Woellner, U. Salzer, D. Pfeifer, H. Veelken, K. Warnatz, F. Tahami, et al. 2009. A homozygous CARD9 mutation in a family with susceptibility to fungal infections. *N. Engl. J. Med.* 361:1727–1735. doi:10.1056/NEJMoa0810719

Guzzo, C., N.F. Che Mat, and K. Gee. 2010. Interleukin-27 induces a STAT1/3- and NF-kappaB-dependent proinflammatory cytokine profile in human monocytes. *J. Biol. Chem.* 285:24404–24411. doi:10.1074/jbc.M110.112599

Herrod, H.G. 1990. Chronic mucocutaneous candidiasis in childhood and complications of non-Candida infection: a report of the Pediatric Immunodeficiency Collaborative Study Group. *J. Pediatr.* 116:377–382. doi:10.1016/S0022-3476(05)82824-0

Hirahara, K., K. Ghoreschi, A. Laurence, X.P. Yang, Y. Kanno, and J.J. O'Shea. 2010. Signal transduction pathways and transcriptional regulation in Th17 cell differentiation. *Cytokine Growth Factor Rev.* 21:425–434. doi:10.1016/j.cytogfr.2010.10.006

Hoshino, A., S. Saint Fleur, and H. Fujii. 2006. Regulation of Stat1 protein expression by phenylalanine 172 in the coiled-coil domain. *Biochem. Biophys. Res. Commun.* 346:1062–1066. doi:10.1016/j.bbrc.2006.06.026

Hunter, C.A. 2005. New IL-12-family members: IL-23 and IL-27, cytokines with divergent functions. *Nat. Rev. Immunol.* 5:521–531. doi:10.1038/nri1648

Kastelein, R.A., C.A. Hunter, and D.J. Cua. 2007. Discovery and biology of IL-23 and IL-27: related but functionally distinct regulators of inflammation. *Annu. Rev. Immunol.* 25:221–242. doi:10.1146/annurev.immunol.22.012703.104758

Kimura, A., T. Naka, K. Nohara, Y. Fujii-Kuriyama, and T. Kishimoto. 2008. Aryl hydrocarbon receptor regulates Stat1 activation and participates in the development of Th17 cells. *Proc. Natl. Acad. Sci. USA.* 105:9721–9726. doi:10.1073/pnas.0804231105

Kirkpatrick, C.H. 2001. Chronic mucocutaneous candidiasis. *Pediatr. Infect. Dis. J.* 20:197–206. doi:10.1097/00006454-200102000-00017

Kisand, K., A.S. Bøe Wolff, K.T. Podkrajsek, L. Tserel, M. Link, K.V. Kisand, E. Ersvaer, J. Perheentupa, M.M. Erichsen, N. Bratanic, et al. 2010. Chronic mucocutaneous candidiasis in APECED or thymoma patients correlates with autoimmunity to Th17-associated cytokines. *J. Exp. Med.* 207:299–308. doi:10.1084/jem.20091669

Kishimoto, T. 2005. Interleukin-6: from basic science to medicine—40 years in immunology. *Annu. Rev. Immunol.* 23:1–21. doi:10.1146/annurev.immunol.23.021704.115806

Kong, X.F., M. Ciancanelli, S. Al-Hajjar, L. Alsina, T. Zumwalt, J. Bustamante, J. Feinberg, M. Audry, C. Prando, V. Bryant, et al. 2010. A novel form of human STAT1 deficiency impairing early but not late responses to interferons. *Blood.* 116:5895–5906. doi:10.1182/blood-2010-04-280586

Kristensen, I.A., J.E. Veirum, B.K. Møller, and M. Christiansen. 2011. Novel STAT1 Alleles in a Patient with Impaired Resistance to Mycobacteria. *J. Clin. Immunol.* 31:265–271. doi:10.1007/s10875-010-9480-8

Levy, D.E., and J.E. Darnell Jr. 2002. Stats: transcriptional control and biological impact. *Nat. Rev. Mol. Cell Biol.* 3:651–662. doi:10.1038/nrm909

Li, H., and R. Durbin. 2009. Fast and accurate short read alignment with Burrows-Wheeler transform. *Bioinformatics.* 25:1754–1760.

Lilic, D. 2002. New perspectives on the immunology of chronic mucocutaneous candidiasis. *Curr. Opin. Infect. Dis.* 15:143–147. doi:10.1097/00001432-200204000-00007

Liu, H., and C. Rohowsky-Kochan. 2011. Interleukin-27-Mediated Suppression of Human Th17 Cells Is Associated with Activation of STAT1 and Suppressor of Cytokine Signaling Protein 1. *J. Interferon Cytokine Res.* 31:459–469. doi:10.1089/jir.2010.0115

Ma, C.S., G.Y. Chew, N. Simpson, A. Priyadarshi, M. Wong, B. Grimbacher, D.A. Fulcher, S.G. Tangye, and M.C. Cook. 2008. Deficiency of Th17 cells in hyper IgE syndrome due to mutations in STAT3. *J. Exp. Med.* 205:1551–1557. doi:10.1084/jem.20080218

McKenna, A., M. Hanna, E. Banks, A. Sivachenko, K. Cibulskis, A. Kernytsky, K. Garimella, D. Altshuler, S. Gabriel, M. Daly, and M.A. DePristo. 2010. The Genome Analysis Toolkit: a MapReduce framework for analyzing next-generation DNA sequencing data. *Genome Res.* 20:1297–1303.

Mertens, C., M. Zhong, R. Krishnaraj, W. Zou, X. Chen, and J.E. Darnell Jr. 2006. Dephosphorylation of phosphotyrosine on STAT1 dimers requires extensive spatial reorientation of the monomers facilitated by the N-terminal domain. *Genes Dev.* 20:3372–3381. doi:10.1101/gad.1485406

Milner, J.D., J.M. Brenchley, A. Laurence, A.F. Freeman, B.J. Hill, K.M. Elias, Y. Kanno, C. Spalding, H.Z. Elloumi, M.L. Paulson, et al. 2008. Impaired T(H)17 cell differentiation in subjects with autosomal dominant hyper-IgE syndrome. *Nature.* 452:773–776. doi:10.1038/nature06764

Minegishi, Y. 2009. Hyper-IgE syndrome. *Curr. Opin. Immunol.* 21:487–492. doi:10.1016/j.coi.2009.07.013

Minegishi, Y., M. Saito, M. Nagasawa, H. Takada, T. Hara, S. Tsuchiya, K. Agematsu, M. Yamada, N. Kawamura, T. Ariga, et al. 2009. Molecular explanation for the contradiction between systemic Th17 defect and localized bacterial infection in hyper-IgE syndrome. *J. Exp. Med.* 206:1291–1301. doi:10.1084/jem.20082767

Ng, S.B., K.J. Buckingham, C. Lee, A.W. Bigham, H.K. Tabor, K.M. Dent, C.D. Huff, P.T. Shannon, E.W. Jabs, D.A. Nickerson, et al. 2010. Exome sequencing identifies the cause of a mendelian disorder. *Nat. Genet.* 42:30–35. doi:10.1038/ng.499

Oppenheim, Y., Y. Ban, and Y. Tomer. 2004. Interferon induced Autoimmune Thyroid Disease (AITD): a model for human autoimmunity. *Autoimmun. Rev.* 3:388–393. doi:10.1016/j.autrev.2004.03.003

Ouyang, W., S. Rutz, N.K. Crellin, P.A. Valdez, and S.G. Hymowitz. 2011. Regulation and functions of the IL-10 family of cytokines in

inflammation and disease. *Annu. Rev. Immunol.* 29:71–109. doi:10.1146/annurev-immunol-031210-101312

Puel, A., R. Döffinger, A. Natividad, M. Chrabieh, G. Barcenas-Morales, C. Picard, A. Cobat, M. Ouachée-Chardin, A. Toulon, J. Bustamante, et al. 2010a. Autoantibodies against IL-17A, IL-17F, and IL-22 in patients with chronic mucocutaneous candidiasis and autoimmune polyendocrine syndrome type I. *J. Exp. Med.* 207:291–297. doi:10.1084/jem.20091983

Puel, A., C. Picard, S. Cypowyj, D. Lilic, L. Abel, and J.L. Casanova. 2010b. Inborn errors of mucocutaneous immunity to Candida albicans in humans: a role for IL-17 cytokines? *Curr. Opin. Immunol.* 22:467–474. doi:10.1016/j.coi.2010.06.009

Puel, A., S. Cypowyj, J. Bustamante, J.F. Wright, L. Liu, H.K. Lim, M. Migaud, L. Israel, M. Chrabieh, M. Audry, et al. 2011. Chronic mucocutaneous candidiasis in humans with inborn errors of interleukin-17 immunity. *Science.* 332:65–68. doi:10.1126/science.1200439

Ramgolam, V.S., Y. Sha, J. Jin, X. Zhang, and S. Markovic-Plese. 2009. IFN-beta inhibits human Th17 cell differentiation. *J. Immunol.* 183:5418–5427. doi:10.4049/jimmunol.0803227

Renner, E.D., S. Rylaarsdam, S. Anover-Sombke, A.L. Rack, J. Reichenbach, J.C. Carey, Q. Zhu, A.F. Jansson, J. Barboza, L.F. Schimke, et al. 2008. Novel signal transducer and activator of transcription 3 (STAT3) mutations, reduced T(H)17 cell numbers, and variably defective STAT3 phosphorylation in hyper-IgE syndrome. *J. Allergy Clin. Immunol.* 122:181–187. doi:10.1016/j.jaci.2008.04.037

Sabat, R. 2010. IL-10 family of cytokines. *Cytokine Growth Factor Rev.* 21:315–324. doi:10.1016/j.cytogfr.2010.11.001

Selmi, C., A. Lleo, M. Zuin, M. Podda, L. Rossaro, and M.E. Gershwin. 2006. Interferon alpha and its contribution to autoimmunity. *Curr. Opin. Investig. Drugs.* 7:451–456.

Shama, S.K., and C.H. Kirkpatrick. 1980. Dermatophytosis in patients with chronic mucocutaneous candidiasis. *J. Am. Acad. Dermatol.* 2:285–294. doi:10.1016/S0190-9622(80)80040-5

Spolski, R., and W.J. Leonard. 2008. Interleukin-21: basic biology and implications for cancer and autoimmunity. *Annu. Rev. Immunol.* 26:57–79. doi:10.1146/annurev.immunol.26.021607.090316

Stumhofer, J.S., A. Laurence, E.H. Wilson, E. Huang, C.M. Tato, L.M. Johnson, A.V. Villarino, Q. Huang, A. Yoshimura, D. Sehy, et al. 2006. Interleukin 27 negatively regulates the development of interleukin 17-producing T helper cells during chronic inflammation of the central nervous system. *Nat. Immunol.* 7:937–945. doi:10.1038/ni1376

Tanaka, K., K. Ichiyama, M. Hashimoto, H. Yoshida, T. Takimoto, G. Takaesu, T. Torisu, T. Hanada, H. Yasukawa, S. Fukuyama, et al. 2008. Loss of suppressor of cytokine signaling 1 in helper T cells leads to defective Th17 differentiation by enhancing antagonistic effects of IFN-gamma on STAT3 and Smads. *J. Immunol.* 180:3746–3756.

Villarino, A.V., E. Gallo, and A.K. Abbas. 2010. STAT1-activating cytokines limit Th17 responses through both T-bet-dependent and -independent mechanisms. *J. Immunol.* 185:6461–6471. doi:10.4049/jimmunol.1001343

Yoshimura, T., A. Takeda, S. Hamano, Y. Miyazaki, I. Kinjyo, T. Ishibashi, A. Yoshimura, and H. Yoshida. 2006. Two-sided roles of IL-27: induction of Th1 differentiation on naive CD4+ T cells versus suppression of proinflammatory cytokine production including IL-23-induced IL-17 on activated CD4+ T cells partially through STAT3-dependent mechanism. *J. Immunol.* 177:5377–5385.

Zhong, M., M.A. Henriksen, K. Takeuchi, O. Schaefer, B. Liu, J. ten Hoeve, Z. Ren, X. Mao, X. Chen, K. Shuai, and J.E. Darnell Jr. 2005. Implications of an antiparallel dimeric structure of nonphosphorylated STAT1 for the activation-inactivation cycle. *Proc. Natl. Acad. Sci. USA.* 102:3966–3971. doi:10.1073/pnas.0501063102

J Clin Immunol (2011) 31:762–772
DOI 10.1007/s10875-011-9560-4

Decreased Expression in Nuclear Factor-κB Essential Modulator Due to a Novel Splice-Site Mutation Causes X-linked Ectodermal Dysplasia with Immunodeficiency

Shuhei Karakawa · Satoshi Okada · Miyuki Tsumura · Yoko Mizoguchi · Norioki Ohno · Shin'ichiro Yasunaga · Motoaki Ohtsubo · Tomoki Kawai · Ryuta Nishikomori · Takemasa Sakaguchi · Yoshihiro Takihara · Masao Kobayashi

Received: 6 March 2011 / Accepted: 14 June 2011 / Published online: 1 July 2011

Abstract X-linked ectodermal dysplasia with immunodeficiency (XL-ED-ID) is caused by hypomorphic mutations in *NEMO*, which encodes nuclear factor-kappaB (NF-κB) essential modulator. We identified a novel mutation, 769−1 G>C, at the splicing acceptor site of exon 7 in *NEMO* in a Japanese patient with XL-ED-ID. Although various abnormally spliced NEMO messenger RNAs (mRNAs) were observed, a small amount of wild-type (WT) mRNA was also identified. Decreased NEMO protein expression was detected in various lineages of leukocytes. Although one abnormally spliced NEMO protein showed residual NF-κB transcription activity, it did not seem to exert a dominant-negative effect against WT-NEMO activity. $CD4^+$ T cell proliferation was impaired in response to measles and mumps, but not rubella. These results were consistent with the clinical and laboratory findings of the patient, suggesting the functional importance of NEMO against specific viral infections. The 769−1 G>C mutation is responsible for decreased WT-NEMO protein expression, resulting in the development of XL-ED-ID.

Keywords NEMO · XL-ED-ID · *IKBKG* · splice-site mutation · measles

Electronic supplementary material The online version of this article (doi:10.1007/s10875-011-9560-4) contains supplementary material, which is available to authorized users.

S. Karakawa · S. Okada (✉) · M. Tsumura · Y. Mizoguchi · N. Ohno · M. Kobayashi
Department of Pediatrics,
Hiroshima University Graduate School of Biomedical Sciences,
1-2-3 Kasumi, Minami-ku,
Hiroshima 734-8551, Japan
e-mail: s-okada@pg8.so-net.ne.jp

S. Yasunaga · M. Ohtsubo · Y. Takihara
Department of Stem Cell Biology, Research Institute for Radiation Biology and Medicine, Hiroshima University,
Hiroshima, Japan

T. Kawai · R. Nishikomori
Department of Pediatrics,
Kyoto University Graduate School of Medicine,
Kyoto, Japan

T. Sakaguchi
Department of Virology,
Hiroshima University Graduate School of Biomedical Sciences,
Hiroshima, Japan

Introduction

X-linked ectodermal dysplasia with immunodeficiency (XL-ED-ID) is an X-linked recessive disease which is characterized by missing or malformed teeth, coarse hair, dry skin, hypohidrosis, and immunodeficiency. It is reportedly caused by mutations in the inhibitor of a kappa light polypeptide gene enhancer in B cells, kinase gamma (*IKBKG*), also called nuclear factor-kappaB (NF-κB) essential modulator (*NEMO*) [1]. NEMO is a subunit of the inhibitor of kappaB (IκB) kinase (IKK) complex and plays pivotal regulatory roles in NF-κB signaling pathways. The IKK complex is activated via NEMO in response to stimulation of a wide range of receptors, including Toll like receptors, CD40, proinflammatory cytokine receptors, ectodysplasin receptor, and receptor activator of NF-κB [2–4]. The activated IKK complex induces ubiquitin-mediated proteasomal degradation of IκB, resulting in translocation of NF-κB dimers from the cytoplasm to the nucleus. Subsequently, NF-κB binds to specific κB sites and regulates target gene transcription, activating downstream

processes involved in inflammation, immunity, cell proliferation, apoptosis, ectodermal formation, and osteogenesis.

Patients with XL-ED-ID are susceptible to multiple and severe bacterial infections of the respiratory and gastrointestinal tracts, skin, soft tissues and bones, together with meningitis and septicemia, from the early stage of infancy [5, 6]. In addition to recurrent severe pyogenic infections, patients also show susceptibility to mycobacterial infections. Although viral infections are not thought to be representative symptoms, some patients suffer from viral infections, e.g., cytomegalovirus (CMV), molluscum contagiosum virus, human papilloma virus, and herpes simplex virus [6, 7]. The immunological abnormalities in the patient with XL-ED-ID are characterized by dysregulated immunoglobulin synthesis or hyperimmunogloblin M (hyper-IgM) syndrome, impaired specific antibody production, defective natural killer (NK) cell activity, and poor proinflammatory cytokine production in response to physiological stimuli. Thus, in patients with XL-ED-ID, responses to various stimuli such as lipopolysaccharide (LPS), interleukin-1 (IL-1), IL-12, IL-18, tumor necrosis factor alpha (TNF-α), and CD40 ligand (CD40L) are impaired [8–11].

Male subjects inheriting large deletions, frameshifts, or other amorphic mutations in *IKBKG* die in utero, indicating that NEMO is essential for development in humans. The mutations in patients with XL-ED-ID are hypomorphic and these mutations impair, but do not abolish NF-κB signaling, thus resulting in distinct clinical and immunological phenotypes.

We identified a novel splice-site mutation, 769−1 G>C, in *IKBKG* in a Japanese boy with XL-ED-ID. This splice-site mutation was shown to produce not only various types of abnormal messenger RNAs (mRNAs), but also low expression of wild-type (WT) mRNA. The expression of WT and abnormal NEMO proteins was also confirmed to be at decreased level in this patient. The decreased expression of NEMO protein is suspected to play an important role in the development of XL-ED-ID.

Methods

Case Report

The patient was a 12-year-old male. He presented with mild mental retardation, conical-shaped teeth, and hypodontia. Hypohidrosis and alopecia were not observed. Similar symptoms were not observed in his family members. He had suffered from recurrent bacterial infections, e.g., three episodes of bacterial meningitis (at 18, 27, and 28 months of age; the pathogenic bacteria isolated from cerebrospinal fluid was *Streptococcus pneumoniae* in the first and third episodes and was unknown in the second episode), recurrent episodes of pneumonia, cellulitis (at 4 years of age; the pathogenic bacteria was unidentified), left knee arthritis (8 years of age, *S. pneumoniae*), and osteomyelitis (12 years old; the pathogenic bacteria was unknown). Furthermore, the patient had also suffered from measles despite receiving a measles vaccination.

The white blood cell and neutrophil counts were both slightly decreased (Table I). The percentage of CD3, CD4, CD8, and CD16/56 in lymphocytes was within the normal range. However, a mild decrease was noted in the $CD19^+$ B cell population. The serum immunoglobulin levels and complement levels were within normal ranges. The production of specific antibodies against *S. pneumoniae* and measles were impaired despite having a history of infections and vaccinations. The specific antibody against *S. pneumoniae* was measured by ELISA and included the antigens of 23 serotypes. He had been vaccinated once with Pneumovax®23 at the age of 9. Furthermore, the specific antibody against the mumps virus was not produced, although the patient was administered the mumps vaccination. However, specific antibodies against CMV, Epstein–Barr virus, Varicella zoster virus, and rubella virus were normally developed. The abdominal ultrasonography examination revealed that the patient's spleen was of normal size. The parents of the patient did not present with immunodeficiency or incontinentia pigmenti.

We obtained blood samples from the patient and healthy adult controls after obtaining informed consent. This study was approved by the Ethics Committee/Internal Review Board of Hiroshima University.

Molecular Genetics

Total RNA was extracted from peripheral blood mononuclear cells (PBMCs). Subsequently, complementary DNA (cDNA) was synthesized by reverse transcription. Polymerase chain reaction (PCR) was performed using primer set 1 (which spans the entire coding region of *IKBKG*, see Supplementary Table) and an Expand Long PCR system (Roche Diagnostics, Germany). The PCR products were sequenced using primer sets 1 and 2. Genomic DNA was extracted from peripheral blood leukocytes and buccal mucosa. Sequence analysis was performed as described previously [12]. In order to investigate the splicing pattern of exon 7, PCR was performed using peripheral blood leukocyte cDNA and primer set 3. The PCR products were cloned into the pGEM-T Easy vector (Promega, USA), and individual alleles were sequenced.

To generate WT and mutant *IKBKG* plasmids, cDNA was synthesized from the patient's PBMCs. PCR was performed using KOD PCR system (TOYOBO, Japan) and primer set 4 (F and R), which includes *Hin*dIII and *Bam*HI sites at the 5′- and 3′-end, respectively, and eliminates the stop codon of *IKBKG*. The PCR products were cloned into the pGEM-

Table I Laboratory data

			RR			Negative range
Leukocyte fraction				Specific antibody		
WBC	5,390	/μl	6,000–10,000	*S. pneumoniae*	Negative	Negative
Neut	1,024	/μl	3,300–7,500	Measles	<8	<8
Ly	3,719	/μl	1,200–4,000	Rubella	>128	<2
Mo	215	/μl	200–950	VZV IgG	40	<10
Eo	377	/μl	0–600	Mumps	<2	<2
Lymphocyte fraction				JEV	<4	<4
CD3	72	%	52–78	CMV IgG	20	<4
CD19	5	%	8–24	EBV VCA IgG	20	<10
CD16/56	21	%	6–27	EBV VCA IgM	<10	<10
CD3/4	38	%	25–48	EBNA	<10	<10
CD3/8	19	%	9–35	Polio type 1, 2, 3	<4	<4
Immunobiochemistry				Pertussis	10	<10
IgG	966	mg/dl	816–1,342	Others		
IgA	292	mg/dl	154-336	NK cell cytotoxicity	6	15–40%
IgM	76	mg/dl	62-103	LTT	Positive	
IgE	54	mg/dl	<100			
CH50	31.2	U/ml	25–48			
C3	97	mg/dl	65–135			
C4	19	mg/dl	13–40			

VZV Varicella zoster virus, *JEV* Japanese encephalitis virus, *CMV* cytomegalovirus, *EBV* Epstein–Barr virus, *EBNA* EBV nuclear antigen, *LTT* lymphocyte transformation test, *RR* reference range

T Easy vector. To generate the construct with a frameshift mutation that produced a premature stop codon, we repeated the PCR to eliminate the original stop codon using primer set 4 (F and R2). These fragments were cloned into P3xFlag-CMV-14 expression vector (Invitrogen, USA) using the *Hin*dIII and *Bam*HI sites.

Reporter Assay

WT and mutant constructs (2 ng per well), IgK-cona-Luc (provided by S. Yamaoka), and pRL-TK (TOYO-B-Net, Japan) were transfected into the NEMO null rat fibroblast cells (provided by S. Yamaoka) using FuGENE HD Transfection Reagent (Roche). We used WT and each of the mutants (1 ng per well, respectively) for co-transfection experiments. At 24 h after transfection, the cells were stimulated with 15 ng/ml LPS (Sigma-Aldrich, USA) for 4 h. Then, cells were subjected to a luciferase assay using the PicaGene Dual Luciferase Assay Kit (TOYO-B-NET). Experiments were done in triplicate and the firefly luciferase activity was normalized to the renilla activity.

Western Blot Analysis

The total proteins from EB virus-transformed B cells (EBV-B cells) were subjected to an immunoblot analysis. We used a mouse anti-NEMO antibody (BD Bioscience, USA) and an anti-flag antibody (Sigma-Aldrich) to detect the NEMO protein and an anti-β-actin antibody (Sigma-Aldrich) as a loading control.

Electrophoretic Mobility Shift Assay

EBV-B cells were stimulated with 10 ng/ml IL-1β (Sigma-Aldrich) for 30 min and subjected to nuclear extraction. We incubated 10 μg of nuclear extract with ^{32}P-labeled (α-dATP) NF-κB probe. The NF-κB double-stranded oligonucleotides corresponding to a NF-κB-binding site consensus sequence 5′-GAT CAT GGG GAA TCC CCA-3′ were used as a NF-κB probe [13].

Flow Cytometry and Carboxyfluorescein Diacetate Succinimidyl Ester Analyses

Flow cytometry analysis of intracellular NEMO protein was performed using the previously reported method [12]. The cells were stained for the following lineage markers after staining for NEMO: CD3, CD14, CD19, and CD56 (BD Bioscience). For CD40L stimulation, PBMCs were cultured with recombinant soluble human CD40L (rCD40L; 2.5 μg/ml; PeproTech Inc, USA) for 48 h and then stained for FCE2 (CD23), ICAM-1 (CD54), Fas (CD95), and CD19

(BD Bioscience). For memory B cell analysis, PBMCs were stained with APC-conjugated anti-CD19, PE-conjugated anti-CD27, and FITC-conjugated anti-IgD antibodies (BD Biosciences). Three-color analysis was carried out by gating on CD19-APC-positive B cells.

For the preparation of measles virus-infected cell lysates (measles lysates), Vero cells were infected with measles virus (the Edmonston strain). Measles lysates were prepared from the cells by clarification with a low-speed centrifugation. The PBMCs from the patient and five healthy adult controls (all were approximately 20 years of age and had developed specific antibodies against measles, rubella, and mumps) were incubated with carboxyfluorescein diacetate succinimidyl ester (CFSE) (Sigma-Aldrich) at a concentration of 0.05 mM [14, 15]. The cells were cultured for 7 days in RPMI-1640 (Sigma-Aldrich) containing 10% AB human serum supplemented with 1 or 3 μg/ml phytohemagglutinin (PHA) (Sigma-Aldrich), 1 or 10 μg/ml measles lysates, 1 or 5 μg/ml rubella lysates (Meridian Life Science, USA), and 1 or 10 μg/ml mumps lysate (Fitzgerald, USA). These cells were stained with APC-conjugated anti-CD4 antibodies (BD Biosciences) and subjected to a flow cytometry analysis.

Cytokine Measurements

We used PBMCs from the patient and four age-matched healthy adult controls (aged 20 years). $CD14^+$ cells were purified from PBMCs using by magnetic sorting (BD Biosciences). The purity levels of $CD14^+$ cells were more than 90%. The $CD14^+$ cells were cultured for 48 h with the addition of 100 U/ml LPS, and the concentration of TNF-α in supernatant was measured in duplicate by Luminex.

Results

A Novel Splice-Site Mutation in *IKBKG* Results in Various Abnormal Splicing Products

High molecular weight DNA was extracted from both the peripheral blood samples and buccal mucosa, and the exons and flanking introns of *IKBKG* were amplified by PCR and sequenced. We identified a novel hemizygous single base-pair G-to-C substitution at nucleotide 769 (−1), 769−1 G>C, of intron 6 in *IKBKG* in the peripheral blood samples (Fig. 1a). The same mutation was also identified in genomic DNA from buccal mucosa, suggesting that this mutation is a germ-line mutation (data not shown). We could not examine the patient's parents and siblings because we could not obtain consent from these family members. Thus, we excluded the possibility that this mutation was a common or irrelevant polymorphism by sequencing 214 healthy

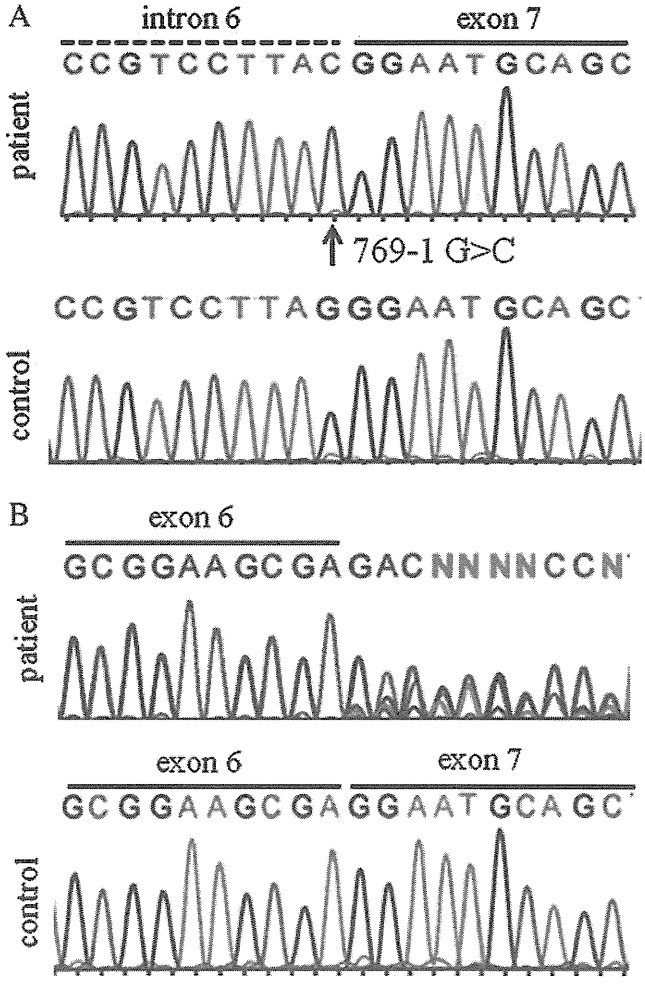

Fig. 1 Sequence analysis. **a** Genomic DNA from the patient and healthy controls were amplified by PCR and the products were analyzed by Sanger sequencing. A novel hemizygous single base-pair G-to-C substitution at nucleotide 769 (−1), 769−1 G>C, was identified in IVS6 of *IKBKG*. **b** Total RNA was extracted from peripheral blood mononuclear cells and cDNA was synthesized by reverse transcription. PCR was performed using primers that spanned the entire coding region of *IKBKG*. The presence of various abnormal splicing variants was predicted in the patient

individuals, including 58 Japanese individuals. A splice junction sequence is highly conserved in eukaryotic cells, which is generally known as a GT-AG rule [16, 17]. Since 769−1 G>C is involved in the highly conserved splicing acceptor site, we analyzed the impact of this mutation on NEMO mRNA splicing. As shown in Fig. 1b, the presence of various abnormal splicing variants was predicted.

In order to investigate the effect of this mutation on splicing, we performed PCR on cDNA with primers which span exons 6 and 7 of *IKBKG*. PCR products were cloned into pGEM-T Easy vector and were subjected to sequence analysis. A sequence analysis of 24 clones demonstrated that 7 clones were derived from normal splicing and the other 17 clones from various abnormal splicing events

(Fig. 2a). Although these abnormal splicing patterns contained insertions and/or deletions in various locations, the major mutant patterns were a 171-bp insertion (+171-NEMO) and 64-bp insertion (+64-NEMO) at the splice acceptor site of exon 7. Among the 17 clones from the abnormal splicing, 13 clones had in-frame changes resulting in large conformational changes of the NEMO protein, and 4 clones (+64-NEMO) were a frameshift change resulting in the premature termination of protein translation (Fig. 2a). The ratio of WT and mutants was similar in PHA- and IL-2-induced T cell blasts which were obtained on the same day (Fig. 2b). We also collected blood samples from the patient on other days, including 1 day the patient was experiencing fever. The ratio of WT to mutant differed in these later samples, compared to those in the initial analysis. In these later timepoints, the ratio of WT was decreased to 5% or 18%, suggesting that the ratio of WT mRNA varies in the patient over time (Fig. 2c, d). To examine whether these splicing variants were also observed in healthy individuals, we tested five healthy individuals and did not find any of the variants found in the patient (representative sequences are shown in Fig. 1b). Altogether, these results suggest that the 769−1 G>C mutation in *IKBKG* is responsible for various abnormal NEMO splicing products.

NEMO Protein Expression Is Decreased in the Patient

In order to examine the effect of the *IKBKG* mutation at the protein level, we analyzed the expression of intracellular NEMO by a flow cytometry analysis. The expression of the NEMO protein in the patient was lower than that in healthy controls in terms of CD3, CD4, CD8, CD56, CD14, and CD19-positive cells (Fig. 3a). Next, we performed an

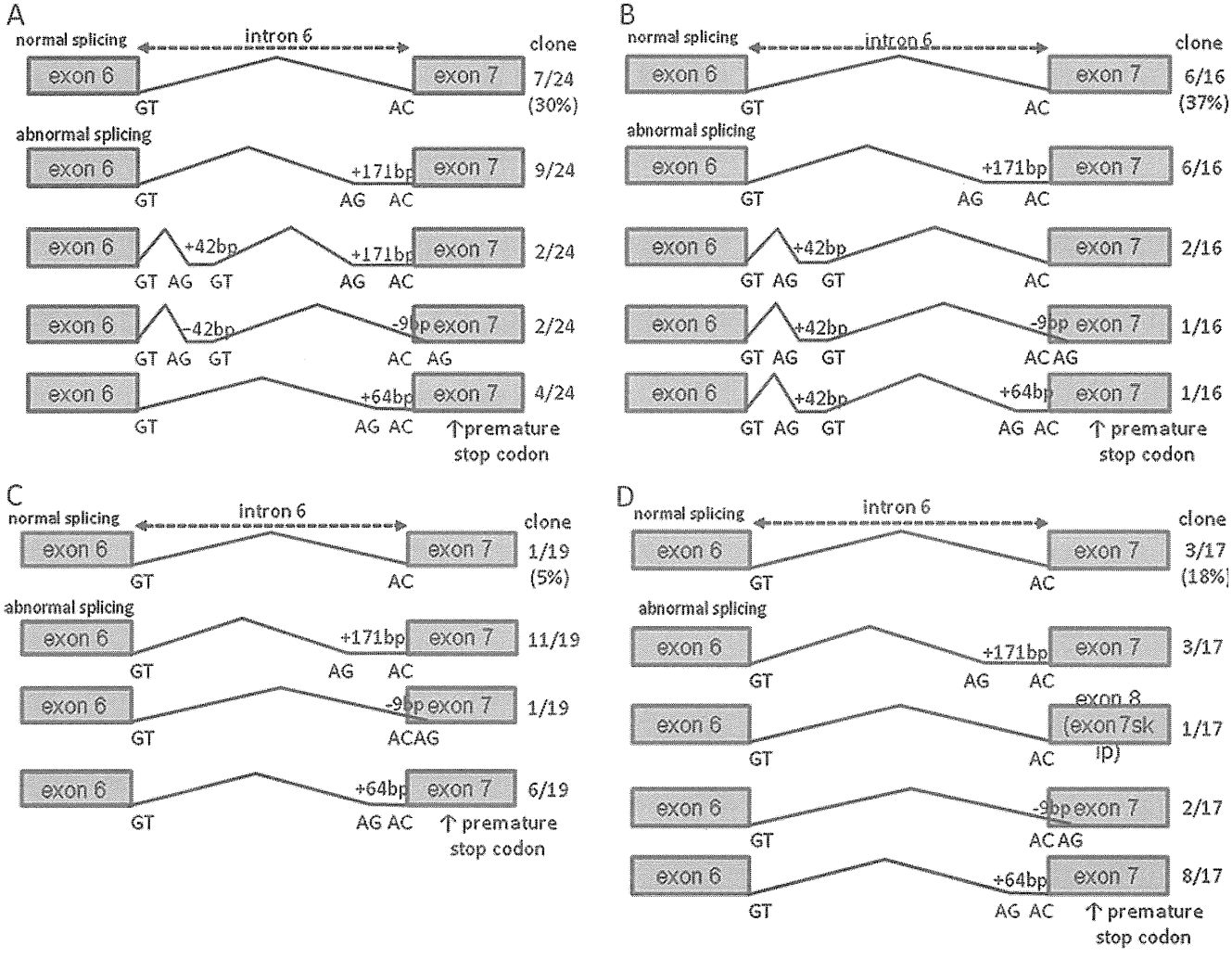

Fig. 2 Cloning analysis. **a** PCR products were cloned into the pGEM-T Easy vector and were subjected to sequence analysis. The splice pattern and the observed number of each clone are shown. The same studies were performed using PHA- and IL-2-induced T cell blasts which were obtained the same day (**b**), PBMCs obtained another day (**c**), and PBMCs obtained on the day the patient was experiencing fever (**d**). The splice pattern and the ratio of WT or mutant variants were different based on the timing of blood collection

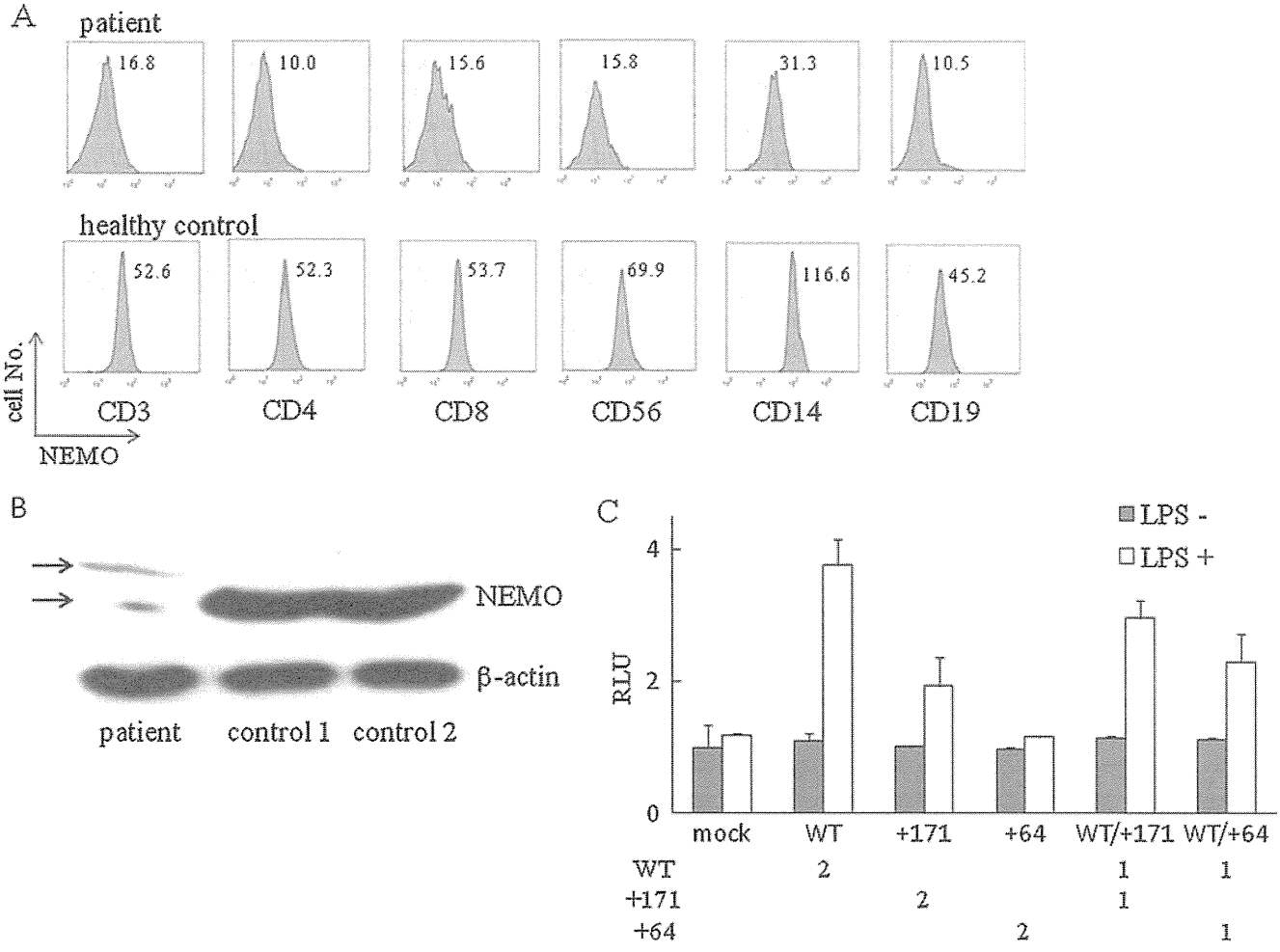

Fig. 3 Analysis of NEMO protein expression and reporter assay. **a** Expression of intracellular NEMO protein from the patient was decreased in various lineages of leukocytes. The geometrical mean fluorescence intensity of NEMO is shown in the FACS profile. **b** EBV-B cells from the patient showed decreased levels of NEMO protein expression. The *upper arrow* shows the band derived from +171-NEMO (approximately 57 kDa), while the *lower arrow* shows WT-NEMO (50 kDa). EBV-B cells in the patient were established from the same blood collection as was used for the cloning analysis of Fig. 2a. **c** WT-, +171-, and +64-NEMO were transfected into NEMO null cells, and NF-κB activity was measured by luciferase assay. The quantity of plasmids (nanogram) used for transfection is described

immunoblot analysis using EBV-B cells from the patient. As shown in Fig. 3b, two major bands were detected, corresponding to the expected molecular weight of the +171-NEMO mutant (approximately 57 kDa) and the known molecular weight of WT-NEMO (50 kDa). The results of densitometry revealed that the expression of WT-NEMO protein from the patient was eightfold lower than that from healthy controls. NEMO mutant proteins derived from other abnormally spliced mRNAs were not detected in this assay.

The Mutant NEMO Proteins Show Decreased NF-κB Transcriptional Activity

To further clarify the characteristics of these abnormally spliced mRNAs, we performed transient gene expression experiments specifically focused on the abnormal splicing products, +171- and +64-NEMO. WT and these mutant constructs were transfected into NEMO null cells. The expression of the WT- and +171-NEMO proteins was detected by either anti-NEMO or anti-Flag antibodies (Supplementary Figure). We were unable to detect the expression of the +64-NEMO protein in the transfectants, suggesting that the +64-NEMO protein may be unstable. Then, we examined the impact of these mutants on NF-κB activation using reporter assay. As shown in Fig. 3c, +64-NEMO abolished NF-κB activation in response to LPS stimulation. On the other hand, +171-NEMO displayed residual NF-κB activity. To further clarify the effect of these mutants on the WT protein, we performed a co-transfection experiment. Co-transfection with half of the amount of WT and +171-NEMO (WT/+171) resulted in only 75% of the

NF-κB activity compared to cells transfected with WT-NEMO, while co-transfection with WT and +64-NEMO (WT/+64) resulted in approximately 50% of WT activity. Considering that +64-NEMO is not expressed at the protein level, the 50% NF-κB activity observed here is likely derived from half the amount of WT-NEMO plasmid. On the other hand, +171-NEMO is thought to have residual activity, even after co-transfection with WT-NEMO. This result suggests that these mutants do not seem to exert a dominant-negative effect against WT-NEMO-mediated NF-κB activation. However, we could not completely rule out the negative effect caused by the other abnormally spliced variants, since we examined only two representative variants.

The Functional Activity via NEMO Is Impaired in the Patient

To analyze the functional impairment caused by the NEMO mutation, we examined the CD23, CD56, and CD95 expression on $CD19^+$ B cells, markers of activated B cells, in response to CD40L stimulation. As shown in Fig. 4a, CD54 and CD95 expressions were reduced compared to healthy controls, and CD23 expression was not detected in the patient's B cells, suggesting that activation of B cells was not completely abrogated in the patient, but instead $CD19^+$ B cells from the patient showed weak levels of activation. Therefore, the patient's cells showed partial, but not complete, impairment following CD40L stimulation. Next, we tested TNF-α production in response to LPS stimulation in peripheral blood $CD14^+$ monocytes. As shown in Fig. 4b, $CD14^+$ monocytes from the patient showed a lower level of TNF-α production compared with those from healthy controls. To further clarify the functional defects, we assessed NF-κB DNA-binding ability in response to IL-1β stimulation using EBV-B cells. As shown in Fig. 4c, NF-κB DNA-binding ability was severely impaired, but not abolished, in the patient. Thus, similar to other patients with XL-ED-ID, the patient's cells also showed impairment in response to various stimuli which induce IKK activation.

Memory B Cells Are Decreased in the Patient

The number of $CD27^+$ memory B cells within the $CD19^+$ B cell population was decreased in the patient (6.0%) in comparison to the number observed in healthy controls (30.4±17.8%, $n=10$). A reduced number of $CD27^+$ memory B cells has also been reported in patients with X-linked anhidrotic ectodermal dysplasia with hyper-IgM syndrome (HED-ID) caused by NEMO impairment [18, 19] as well as in a patient with a 5′ untranslated region (UTR) mutation of *IKBKG*, with high levels of IgA [20]. However, as far as we know, a reduction in the memory B cell compartment has not yet been reported in patients with ED-ID. B cells in patients with defect in NF-κB are unable to undergo somatic hypermutation and class switch recombination, resulting in a loss of memory B cells [19, 21, 22]. Although we need to test other patients with ED-ID to confirm this memory B cell phenotype, the diminished memory B cell population may become a common finding not only in patients with HED-ID, but also in patients with an impairment of NEMO.

The Increase in $CD4^+$ T Cell Proliferation Is Impaired for Measles and Mumps Infections

The patient developed measles in spite of having a history of measles vaccination. Furthermore, although specific antibodies against measles and mumps virus were not detected, specific antibodies against CMV, Epstein–Barr virus, Varicella zoster virus, and rubella virus were normal. To clarify the mechanism underlying the impairment of specific antibody production against measles and mumps viruses, we tested the specific T cell response against these viral infections. We analyzed $CD4^+$ T cells using a CFSE proliferation assay according to the method described in a previous report [23]. $CD4^+$ T cells from the patient were unable to proliferate in response to measles lysate and mumps lysate (Fig. 5a, b). On the other hand, they proliferated well in response to PHA and rubella lysate. CFSE is a commonly used and useful tool for analyzing specific T cell response against *Candida*, CMV, measles viruses, and others, and these results suggest that the specific T cell response against measles and mumps virus is impaired in the patient [14, 15, 23]. These findings were compatible with patient's laboratory findings of the impairment of a specific antibody production against measles virus and mumps virus, in spite of having received these vaccinations and having a prior measles infection.

Discussion

We identified a novel hemizygous splice-site mutation in *IKBKG* in a Japanese boy with XL-ED-ID. Both the WT and various abnormally spliced forms of NEMO mRNA were observed in the patient's cells. There are two possibilities which may account for this finding. One is leakage through the splice-site mutation, the other is mosaicism. Leakage through the splice-site mutation has also been described in many human diseases [24–26], including in a patient with a NEMO abnormality who had a splice-site mutation, 1056−1 G>A [27]. Similar to what was observed in our current study, the ratio of WT to mutant NEMO mRNA observed varied with the timing of blood

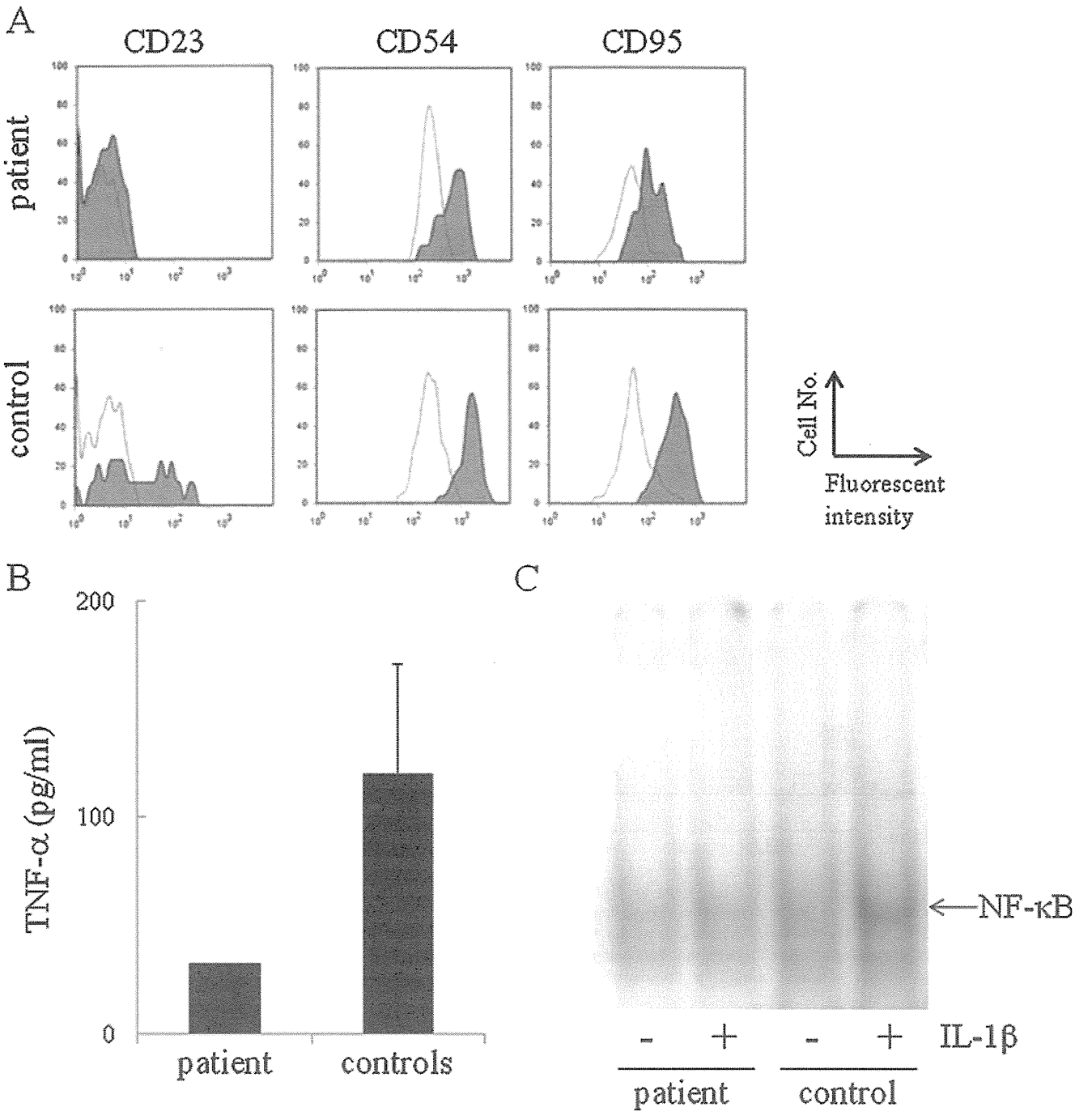

Fig. 4 Analysis of functional activity via NEMO. **a** Expression of CD23, CD54, and CD95, the surface markers of activated B cells, was measured using flow cytometry. PBMCs from the patient and healthy controls were treated with (*shaded histograms*) or without (*open histograms*) CD40L. **b** TNF-α production in response to LPS by $CD14^+$ cells was measured by Luminex. Data from the healthy subjects are represented as mean ± SD (n=4). **c** The NF-κB DNA-binding ability in response to IL-1β was measured by electrophoretic mobility shift assay. EBV-B cells from the patient showed a lower level of DNA-binding ability than healthy controls

collection in the patient with a 1056−1 G>A mutation. Curiously, however, there is a difference between the expression of WT-NEMO protein and the frequency of WT-NEMO mRNA in our patient. Although the frequency of WT-NEMO mRNA observed in the patient in our splicing assay was approximately 30% of all splice transcripts, expression of NEMO protein from the patient was only 12.5% that of WT levels. We suspect that the influence of nonsense-mediated RNA decay can explain this inconsistency between WT-NEMO expression at the mRNA and protein level. Some abnormally spliced forms of NEMO, such as 64-NEMO, result in premature stop codon. These

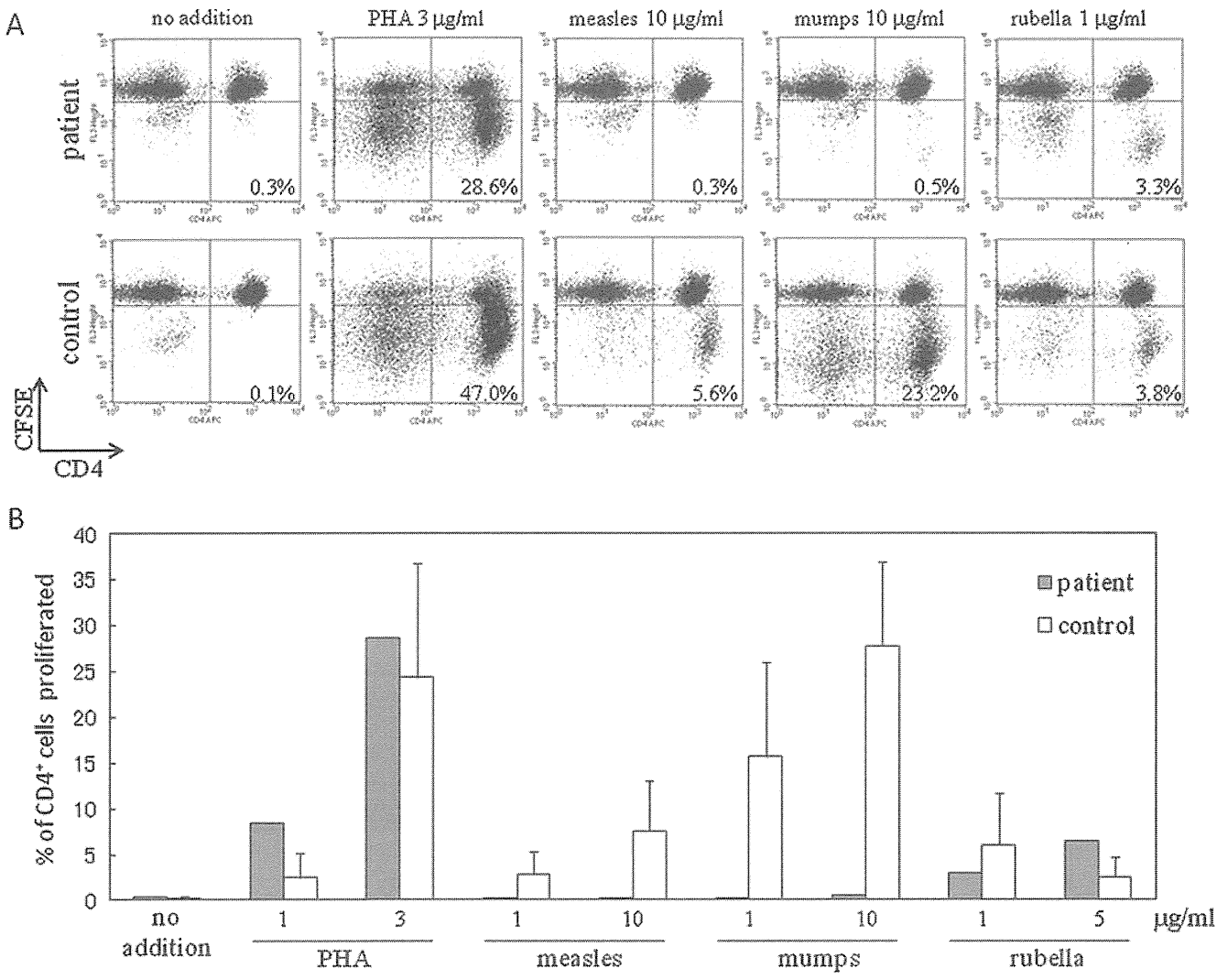

Fig. 5 CFSE analysis of the response of $CD4^+$ cells to PHA and various viruses. **a** Representative FACS figures from the patient and healthy subjects are shown. The *lower-right quadrant* of the FACS profile indicates the proportion of $CD4^+$ T cells that had undergone division in response to the indicated stimuli. **b** Summary of the percentage of proliferating $CD4^+$ T cells is shown. The data in the *white columns* represent the mean ± SD of five healthy subjects. Although $CD4^+$ T cells from the patient proliferated in response to the rubella virus, few divided cells were observed upon stimulation with the measles or mumps viruses

products are predicted to be susceptible to nonsense-mediated RNA decay. Therefore, although the splicing assay in this study is an effective way to detect variously spliced transcripts derived from the 769−1 G>C mutation, it may overestimate the proportion of in-frame transcripts which include WT-NEMO.

The other possibility to explain the existence of both WT and mutant mRNAs is germ-line or reversion mosaicism of WT and mutant NEMO-containing cells, as has previously been reported in patients with immunological disorders [28–31]. Furthermore, a reversion mosaicism has been identified in one patient with XL-ED-ID [12]. This patient exhibited NEMO protein expression that varied among cell lineages. Two types of NEMO-expressing cells, NEMO high and NEMO low, were observed by flow cytometric analysis. However, the pattern of NEMO expression did not differ among the lineages in our current study (Fig. 3a). In addition, we did not identify the WT-NEMO sequence from Sanger sequence using genomic DNA extracted from peripheral blood leukocytes or buccal mucosa from the patient (Fig. 1a). Taken together, although we could not completely exclude the possibility of low frequency mosaicism, we presume that normal NEMO mRNAs are derived from leakage through the splice-site mutation that may give rise to XL-ED-ID.

The levels of NEMO protein expression decreased markedly, and the functional activity via NEMO in response to various stimuli were impaired in our patient. Recently, Mooster et al. reported a patient with immunodeficiency caused by a splice-site mutation in the 5′ UTR of the

IKBKG [20]. This patient also showed decreased expression of the NEMO protein, thus resulting in reduced NF-κB activity. In addition, the authors proposed that inadequate levels of normal NEMO protein played a role in the molecular pathogenesis of this patient. Similarly, decreased expression of NEMO protein was also suspected to have played an important role in the clinical manifestations of our patient. However, in contrast to our patient, neither the patients with 1056−1 G>C nor 5′ UTR mutation that demonstrated a residual expression of WT-NEMO presented with ectodermal dysplasia. Further studies will therefore be required to elucidate the factor that is associated with the development of the ectodermal phenotype.

$CD4^+$ T cells from the patient exhibit impaired proliferation in response to measles and mumps viruses. On the other hand, normal proliferation was observed upon stimulation with the rubella virus. To our knowledge, this is the first study to clarify an impairment of T cell proliferation in response to viral infections by CSFE analysis in a patient with NEMO mutation. These results were completely consistent with the laboratory finding of specific antibody production against rubella, but not measles and mumps viruses. Furthermore, the impairment of antibody production against measles, but not rubella, was also observed in another patient with ED-ID carrying a D311E hypomorphic mutation in *NEMO* (Imai et al., in revision in J Clin Immunol). It is interesting to speculate how the impairment of the NEMO protein disturbs the response against measles. Generally, the first line of host defense against viral infection is the innate immune system [32]. Viral infections induce inflammatory reactions via induction of IFNs and via the activation of NF-κB. The activation of interferon regulatory factor-3 (IRF-3) plays an important role in the induction of IFNs against viral infections. IRF-3 recognizes the measles virus nucleocapsid and triggers the induction of interferon production. However, IRF-3 activation and IRF-3-dependent gene induction are abrogated in NEMO-deficient cells [33]. Indeed, impairment of TLR3-induced NF-κB- and IRF-3-dependent IFN induction has also been documented in a patient with NEMO mutation (Audry et al. J Allergy Clin Immunol. in press, reference number: YMAI 8998). In addition, the activation of NF-κB also plays a pivotal role in the host defense against measles. The measles virus phosphoprotein upregulates the ubiquitin-modifying enzyme A20, a negative feedback regulator of NF-κB, resulting in viral escape from the host immune system [34, 35]. Therefore, the impairments of acquired immunity against viral infections observed in the patient may be derived from an impairment of innate immunity caused by NEMO mutation. Further studies will therefore be required to confirm the clinical and cellular phenotype against viral infections in other patients with NEMO mutation.

Conclusion

The 769−1 G>C mutation was shown to cause a decrease in NF-κB activation through the decreased expression level of NEMO protein, thus resulting in the development of XL-ED-ID.

Acknowledgments This work was supported by a Grant-in-Aid for Young Scientist (B) No. 20790731 from Japan Society for the Promotion of Science. This work was also supported by the grants from the Japanese Ministry of Education, Culture, Sports, and Technology and grants from the Japanese Ministry of Health, Labor, and Welfare. We wish to thank the Analysis Center of Life Science, Hiroshima University for the use of their facilities. We also thank Natsuki Nabe and Yuki Takaoka for their valuable help with the reporter assay.

References

1. Doffinger R, Smahi A, Bessia C, Geissmann F, Feinberg J, Durandy A, et al. X-linked anhidrotic ectodermal dysplasia with immunodeficiency is caused by impaired NF-kappaB signaling. Nat Genet. 2001;27:277–85.
2. Fusco F, Pescatore A, Bal E, Ghoul A, Paciolla M, Lioi MB, et al. Alterations of the IKBKG locus and diseases: an update and a report of 13 novel mutations. Hum Mutat. 2008;29:595–604.
3. Puel A, Picard C, Ku CL, Smahi A, Casanova JL. Inherited disorders of NF-kappaB-mediated immunity in man. Curr Opin Immunol. 2004;16:34–41.
4. Courtois G, Smahi A, Israel A. NEMO/IKK gamma: linking NF-kappa B to human disease. Trends Mol Med. 2001;7:427–30.
5. Hanson EP, Monaco-Shawver L, Solt LA, Madge LA, Banerjee PP, May MJ, et al. Hypomorphic nuclear factor-kappaB essential modulator mutation database and reconstitution system identifies phenotypic and immunologic diversity. J Allergy Clin Immunol. 2008;122:1169–77.
6. Orange JS, Jain A, Ballas ZK, Schneider LC, Geha RS, Bonilla FA. The presentation and natural history of immunodeficiency caused by nuclear factor kappaB essential modulator mutation. J Allergy Clin Immunol. 2004;113:725–33.
7. Lee WI, Torgerson TR, Schumacher MJ, Yel L, Zhu Q, Ochs HD. Molecular analysis of a large cohort of patients with the hyper immunoglobulin M (IgM) syndrome. Blood. 2005;105:1881–90.
8. Filipe-Santos O, Bustamante J, Haverkamp MH, Vinolo E, Ku CL, Puel A, et al. X-linked susceptibility to mycobacteria is caused by mutations in NEMO impairing CD40-dependent IL-12 production. J Exp Med. 2006;203:1745–59.
9. Orange JS, Brodeur SR, Jain A, Bonilla FA, Schneider LC, Kretschmer R, et al. Deficient natural killer cell cytotoxicity in patients with IKK-gamma/NEMO mutations. J Clin Invest. 2002;109(11):1501–9.
10. Vinolo E, Sebban H, Chaffotte A, Israel A, Courtois G, Veron M, et al. A point mutation in NEMO associated with anhidrotic ectodermal dysplasia with immunodeficiency pathology results in destabilization of the oligomer and reduces lipopolysaccharide- and tumor necrosis factor-mediated NF-kappa B activation. J Biol Chem. 2006;281:6334–48.
11. Smahi A, Courtois G, Rabia SH, Doffinger R, Bodemer C, Munnich A, et al. The NF-kappaB signalling pathway in human diseases: from incontinentia pigmenti to ectodermal dysplasias and immune-deficiency syndromes. Hum Mol Genet. 2002;11:2371–5.

12. Nishikomori R, Akutagawa H, Maruyama K, Nakata-Hizume M, Ohmori K, Mizuno K, et al. X-linked ectodermal dysplasia and immunodeficiency caused by reversion mosaicism of NEMO reveals a critical role for NEMO in human T-cell development and/or survival. Blood. 2004;103:4565–72.
13. Puel A, Reichenbach J, Bustamante J, Ku CL, Feinberg J, Doffinger R, et al. The NEMO mutation creating the most-upstream premature stop codon is hypomorphic because of a reinitiation of translation. Am J Hum Genet. 2006;78:691–701.
14. Fazekas de St Groth B, Smith AL, Koh WP, Girgis L, Cook MC, Bertolino P. Carboxyfluorescein diacetate succinimidyl ester and the virgin lymphocyte: a marriage made in heaven. Immunol Cell Biol. 1999;77:530–8.
15. Lyons AB. Analysing cell division in vivo and in vitro using flow cytometric measurement of CFSE dye dilution. J Immunol Methods. 2000;243:147–54.
16. Mount SM. A catalogue of splice junction sequences. Nucleic Acids Res. 1982;10:459–72.
17. Mount SM. Genomic sequence, splicing, and gene annotation. Am J Hum Genet. 2000;67:788–92.
18. Jain A, Ma CA, Liu S, Brown M, Cohen J, Strober W. Specific missense mutations in NEMO result in hyper-IgM syndrome with hypohydrotic ectodermal dysplasia. Nat Immunol. 2001;2:223–8.
19. Jain A, Ma CA, Lopez-Granados E, Means G, Brady W, Orange JS, et al. Specific NEMO mutations impair CD40-mediated c-Rel activation and B cell terminal differentiation. J Clin Invest. 2004;114:1593–602.
20. Mooster JL, Cancrini C, Simonetti A, Rossi P, Di Matteo G, Romiti ML, et al. Immune deficiency caused by impaired expression of nuclear factor-kappaB essential modifier (NEMO) because of a mutation in the 5′ untranslated region of the NEMO gene. J Allergy Clin Immunol. 2010;126:127–32.
21. Kouskoff V, Nemazee D. Role of receptor editing and revision in shaping the B and T lymphocyte repertoire. Life Sci. 2001;69:1105–13.
22. Souto-Carneiro MM, Fritsch R, Sepulveda N, Lagareiro MJ, Morgado N, Longo NS, et al. The NF-kappaB canonical pathway is involved in the control of the exonucleolytic processing of coding ends during V(D)J recombination. J Immunol. 2008;180:1040–9.
23. Munier CM, Zaunders JJ, Ip S, Cooper DA, Kelleher AD. A culture amplified multi-parametric intracellular cytokine assay (CAMP-ICC) for enhanced detection of antigen specific T-cell responses. J Immunol Methods. 2009;345:1–16.
24. Arredondo-Vega FX, Santisteban I, Kelly S, Schlossman CM, Umetsu DT, Hershfield MS. Correct splicing despite mutation of the invariant first nucleotide of a 5′ splice site: a possible basis for disparate clinical phenotypes in siblings with adenosine deaminase deficiency. Am J Hum Genet. 1994;54:820–30.
25. Krawczak M, Reiss J, Cooper DN. The mutational spectrum of single base-pair substitutions in mRNA splice junctions of human genes: causes and consequences. Hum Genet. 1992;90:41–54.
26. Seyama K, Nonoyama S, Gangsaas I, Hollenbaugh D, Pabst HF, Aruffo A, et al. Mutations of the CD40 ligand gene and its effect on CD40 ligand expression in patients with X-linked hyper IgM syndrome. Blood. 1998;92:2421–34.
27. Orange JS, Levy O, Brodeur SR, Krzewski K, Roy RM, Niemela JE, et al. Human nuclear factor kappa B essential modulator mutation can result in immunodeficiency without ectodermal dysplasia. J Allergy Clin Immunol. 2004;114:650–6.
28. Arveiler B, de Saint-Basile G, Fischer A, Griscelli C, Mandel JL. Germ-line mosaicism simulates genetic heterogeneity in Wiskott–Aldrich syndrome. Am J Hum Genet. 1990;46:906–11.
29. Hirschhorn R, Yang DR, Puck JM, Huie ML, Jiang CK, Kurlandsky LE. Spontaneous in vivo reversion to normal of an inherited mutation in a patient with adenosine deaminase deficiency. Nat Genet. 1996;13:290–5.
30. Wada T, Schurman SH, Otsu M, Garabedian EK, Ochs HD, Nelson DL, et al. Somatic mosaicism in Wiskott–Aldrich syndrome suggests in vivo reversion by a DNA slippage mechanism. Proc Natl Acad Sci U S A. 2001;98:8697–702.
31. Stephan V, Wahn V, Le Deist F, Dirksen U, Broker B, Muller-Fleckenstein I, et al. Atypical X-linked severe combined immunodeficiency due to possible spontaneous reversion of the genetic defect in T cells. N Engl J Med. 1996;335:1563–7.
32. Yokota S, Okabayashi T, Fujii N. The battle between virus and host: modulation of Toll-like receptor signaling pathways by virus infection. Mediators Inflamm. 2010;2010:184328.
33. Zhao T, Yang L, Sun Q, Arguello M, Ballard DW, Hiscott J, et al. The NEMO adaptor bridges the nuclear factor-kappaB and interferon regulatory factor signaling pathways. Nat Immunol. 2007;8:592–600.
34. Indoh T, Yokota S, Okabayashi T, Yokosawa N, Fujii N. Suppression of NF-kappaB and AP-1 activation in monocytic cells persistently infected with measles virus. Virology. 2007;361:294–303.
35. Yokota S, Okabayashi T, Yokosawa N, Fujii N. Measles virus P protein suppresses Toll-like receptor signal through up-regulation of ubiquitin-modifying enzyme A20. FASEB J. 2008;22:74–83.

In conclusion, the associations among asthma, biofilm-forming bacteria, and revision ESS are strong and robust after adjusting for other factors in patients with CRS from a tertiary medical center. Despite its limitations, this study may improve our understanding of refractory CRS pathogenesis, possibly leading to more effective treatment strategies, such as incorporating the treatments of asthma and biofilm infection into conventional CRS therapies. Prospective cohort studies in diverse populations are needed to assess the causality of these associations.

We thank Alexander Chiu for providing the clinical samples, Andrew Cucchiara for helping with the data cleansing and analysis, and Jennifer Kofonow, Anthony Prince, Jacob Steiger, Michael Cohen, Edwin Tamashiro, and Natalia Goldstein for performing the Calgary biofilm assay and organizing the data.

Zi Zhang, MD[a]
Darren R. Linkin, MD, MSCE[b]
Brian S. Finkelman, BS[a]
Bert W. O'Malley, Jr, MD[c]
Erica R. Thaler, MD[c]
Laurel Doghramji, RN, BSN[c]
David W. Kennedy, MD[c]
Noam A. Cohen, MD, PhD[c]
James N. Palmer, MD[c]

From [a]the Center for Clinical Epidemiology and Biostatistics, [b]the Department of Medicine, Division of Infectious Diseases, and [c]the Department of Otorhinolaryngology–Head and Neck Surgery, University of Pennsylvania School of Medicine, Philadelphia, Pa. E-mail: james.palmer@uphs.upenn.edu.

Supported by the Flight Attendant Medical Research Institute Clinical Investigator Award (053367 to N.A.C. and 052414 to J.N.P.).

Disclosure of potential conflict of interest: J. N. Palmer receives research support from the Flight Attendant Medical Research Institute, has provided legal consultation/expert witness testimony in cases related to complications in sinus surgery, and is a member of the board of directors for the American Rhinologic Society. D. W. Kennedy is the medical director of ENT Care and a member of RhinActive. N. A. Cohen receives research support from the Flight Attendant Medical Research Institute. The rest of the authors have declared that they have no conflict of interest.

REFERENCES

1. Fokkens W, Lund V, Mullol J. EP3OS 2007: European position paper on rhinosinusitis and nasal polyps 2007: a summary for otorhinolaryngologists. Rhinology 2007; 45:97-101.
2. Newman LJ, Platts-Mills TA, Phillips CD, Hazen KC, Gross CW. Chronic sinusitis: relationship of computed tomographic findings to allergy, asthma, and eosinophilia. JAMA 1994;271:363-7.
3. Psaltis AJ, Weitzel EK, Ha KR, Wormald PJ. The effect of bacterial biofilms on post-sinus surgical outcomes. Am J Rhinol 2008;22:1-6.
4. Prince AA, Steiger JD, Khalid AN, Dogrhamji L, Reger C, Eau Claire S, et al. Prevalence of biofilm-forming bacteria in chronic rhinosinusitis. Am J Rhinol 2008;22: 239-45.
5. Meltzer EO, Hamilos DL, Hadley JA, Lanza DC, Marple BF, Nicklas RA, et al. Rhinosinusitis: establishing definitions for clinical research and patient care. J Allergy Clin Immunol 2004;114:155-212.
6. National Asthma Education and Prevention Program. Expert Panel Report 3 (EPR-3): guidelines for the diagnosis and management of asthma-summary report 2007. J Allergy Clin Immunol 2007;120:S94-S138.
7. Banerji A, Piccirillo JF, Thawley SE, Levitt RG, Schechtman KB, Kramper MA, et al. Chronic rhinosinusitis patients with polyps or polypoid mucosa have a greater burden of illness. Am J Rhinol 2007;21:19-26.
8. Costerton JW, Stewart PS, Greenberg EP. Bacterial biofilms: a common cause of persistent infections. Science 1999;284:1318-22.
9. Richtsmeier WJ. Top 10 reasons for endoscopic maxillary sinus surgery failure. Laryngoscope 2001;111:1952-6.

Available online March 24, 2011.
doi:10.1016/j.jaci.2011.02.022

Quantification of κ-deleting recombination excision circles in Guthrie cards for the identification of early B-cell maturation defects

To the Editor:

X-linked agammaglobulinemia (XLA) is a primary immunodeficiency caused by severely decreased numbers of mature peripheral B lymphocytes as a result of a mutation in the *BTK* gene. Non-XLA is characterized by hypogammaglobulinemia with decreased B-cell counts (less than 2% of mature B cells) in the absence of the *BTK* gene mutation. Both XLA and non-XLA are caused by an early B-cell maturation defect.[1] In patients with XLA and non-XLA, recurrent infections appear between 3 and 18 months of age, whereas the mean age at diagnosis is 3 years.[2] This delayed diagnosis results in frequent hospitalization because of pneumonia, sepsis, meningitis, and other bacterial infections, which frequently require intravenous administration of antibiotics and can be fatal. Frequent pneumonia results in a high incidence of chronic lung diseases.[3] Thus, early diagnosis and early treatment, including periodical intravenous immunoglobulin replacement therapy, is essential to improve the prognosis and the quality of life of patients with XLA and non-XLA.

In the process of B-cell maturation, immunoglobulin κ-deleting recombination excision circles (KRECs) are produced during κ-deleting recombination allelic exclusion and isotypic exclusion of the λ chain.[4] Coding joint (cj) KRECs reside within the chromosome, whereas signal joint (sj) KRECs are excised from genomic DNA. cjKREC levels remain the same after B-cell division, whereas sjKREC levels decrease, because sjKRECs are not replicated during cell division.[5] Because the B-cell maturation defects in XLA and non-XLA occur before κ-deleting recombination, KRECs are not supposed to be produced. Therefore, measurements of KRECs have the potential to be applied to the identification of these types of B-cell deficiencies in patients, which consist of around 20% of all B-cell defects.[6] In addition, some types of combined immunodeficiencies show an arrest in B-cell maturation and can also be identified by this method. The success of newborn screening for T-cell deficiencies by measuring T-cell–receptor excision circles[7] prompted us to develop a newborn screening method for XLA and non-XLA by measuring KRECs derived from neonatal Guthrie cards.

The study protocol was approved by the National Defense Medical College institutional review board, and written informed consent was obtained from the parents of normal controls, the affected children, and adult patients, in accordance with the Declaration of Helsinki.

First, we determined the sensitivity of detection levels of cjKRECs and sjKRECs in Guthrie cards using real-time quantitative PCR.[5] Normal B cells from a healthy adult were isolated from peripheral blood (PB; mean purity, 88.5%). PB was also obtained from 1 patient with XLA (P20) whose B-cell number was 0.09 in 1 μL whole blood and who was negative for sjKRECs ($<1.0 \times 10^2$ copies/μg DNA). Various numbers of normal B cells were serially added to 1 mL whole PB obtained from this patient with XLA. The B-cell–added XLA whole blood was then applied to filter papers, and 3 punches (3 mm in diameter) of dried blood spots were used for DNA extraction. At least 3 DNA samples containing the same B-cell concentrations (0.09-400 B cells/μL) were used for the real-time quantitative PCR of cjKRECs and sjKRECs. The percentages of the positive samples ($>1.0 \times 10^2$ copies/μg DNA) of cjKRECs and sjKRECs increased constantly

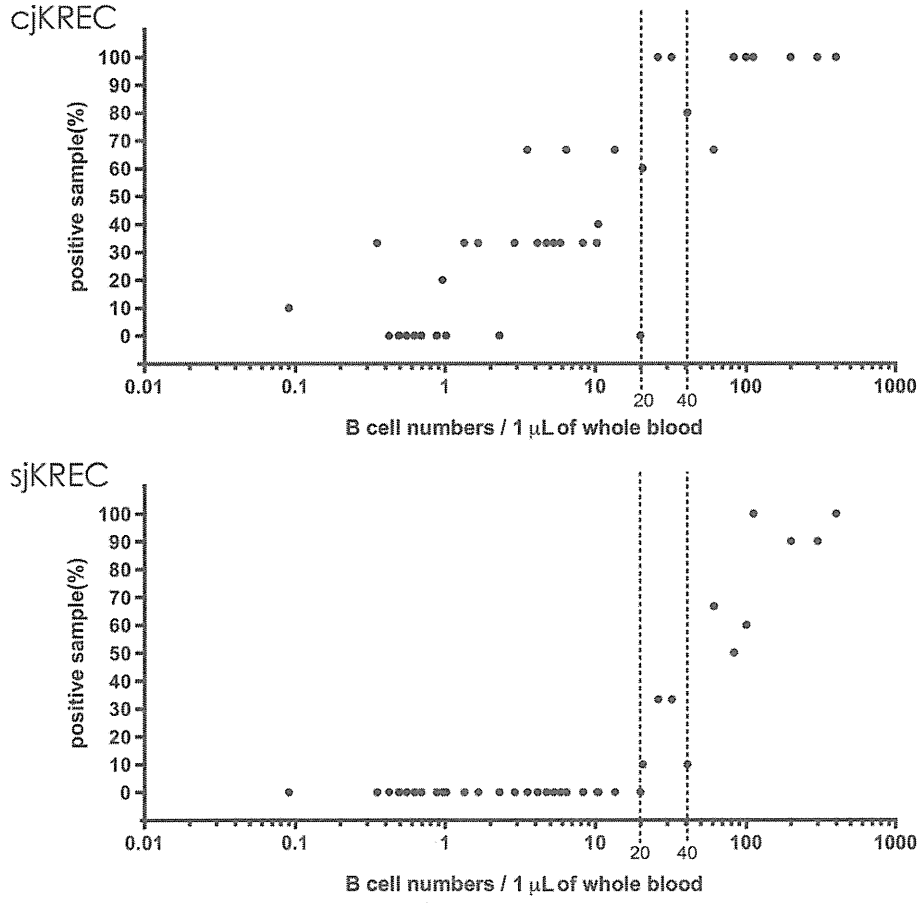

FIG 1. Sensitivity levels of cjKRECs and sjKRECs. Various numbers of purified normal B cells were serially added to whole PB from a patient with XLA (P20) to obtain B-cell–added XLA whole blood. cjKRECs and sjKRECs were measured in 3 to 10 samples of each concentration in triplicate. In all analyses, RNaseP (internal control) was positive ($2.3 \pm 0.2 \times 10^5$ copies/μg DNA). *X-axis,* B-cell numbers in 1 μL whole blood from a patient with XLA. *Y-axis,* Percentages of the KREC-positive results in the tests.

as the B-cell concentrations increased (Fig 1). None of the samples were positive for sjKRECs when the B-cell numbers were less than 20/μL, but cjKRECs were often positive. It has been reported that 90% of patients with XLA have less than 0.2% B cells in the PB at diagnosis.[1] Because peripheral lymphocyte numbers in neonates range from 1200 to 9800/μL,[8] the absolute B-cell numbers of 90% of patients with XLA are estimated to be 2.4 to 19.6/μL at the time of blood collection for Guthrie cards, although exact B-cell numbers of XLA in neonatal periods are not known at this moment. Because neonates are known to have fewer B cells than infants,[9] and we observed that B-cell numbers are constantly low in patients with XLA throughout infancy (Nakagawa, unpublished data, June 2010), which is consistent with the fact that BTK plays an essential role in B-cell maturation. It is likely that neonates with XLA also have severely decreased B cells. On the other hand, all samples obtained from 400 B cells/μL were positive for both cjKRECs and sjKRECs. We also observed that all healthy infants (1-11 months old; n = 15) were sjKREC-positive (Nakagawa, unpublished data, June 2010) and might have at least 600 B cells/μL whole blood.[9] From these data, it is assumed that at least 90% of patients with XLA are sjKREC-negative, and healthy neonates are positive for sjKRECs on neonatal Guthrie cards.

Next, we measured cjKRECs and sjKRECs in dried blood spots in filter papers or Guthrie cards from 30 patients with XLA and 5 patients with non-XLA and from 133 neonates born at the National Defense Medical College Hospital during this study period (August 2008 to October 2009) and 138 healthy subjects of various ages (1 month to 35 years old) to investigate the validity of this method. The levels of B cells of the patients ranged from 0.0% to 1.1% of total lymphocytes and 0.0 to 35.78/μL. IgG levels were 10 to 462 mg/dL (see this article's Tables E1 and E2 in the Online Repository at www.jacionline.org). Patients with leaky phenotypes[1,10] were included; 1 patient (P30) had more than 1% B cells and 34.22/μL total B cells, and 4 patients had more than 300 mg/dL serum IgG (P12, P30, P31, P33). All of the normal neonatal Guthrie cards were positive for both cjKRECs and sjKRECs ($7.2 \pm 0.7 \times 10^3$ and $4.8 \pm 0.6 \times 10^3$ copies/μg DNA, respectively). All healthy subjects of various ages were also positive for both cjKRECs and sjKRECs (Nakagawa, unpublished data, June 2010). In contrast, specimens from all 35 B-cell–deficient patients were sjKREC-negative ($<1.0 \times 10^2$ copies/μg DNA; Fig 2). All 5 patients with leaky phenotypes were also sjKREC-negative, which might be explained by the hypothesis that leaky B cells of patients with XLA are long-lived B cells that divided several times and have fewer sjKRECs than naive B cells.

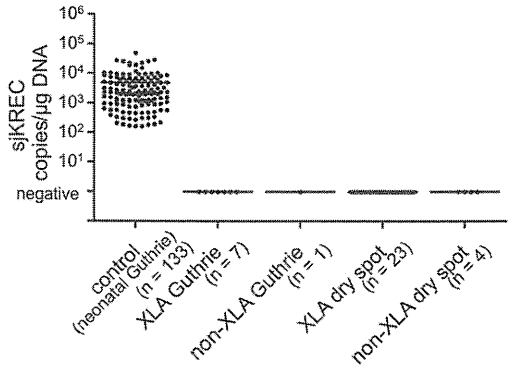

FIG 2. Copy numbers of sjKRECs measured in neonatal Guthrie cards or dried blood spots obtained from B-cell–deficient patients. On all samples from control, neonatal Guthrie cards (n = 133) were sjKREC-positive (4.8 ± 0.6 × 10^3 copies/μg DNA). B-cell–deficient patients were negative for sjKRECs in neonatal Guthrie cards (XLA, n = 7; non-XLA, n = 1) and dried blood spots (XLA, n = 23; non-XLA, n = 4).

One patient (P27) was positive for cjKRECs, but other patients were negative for it. *RPPH1* (internal control) was detectable at the same level as in normal controls in all samples.

These results indicate that sjKRECs are undetectable in XLA and non-XLA and suggest that measurement of sjKRECs in neonatal Guthrie cards has the potential for the use of newborn mass screening to identify neonates with early B-cell maturation defects. Greater numbers of neonatal Guthrie cards should be examined to confirm this potential, and the data obtained from dried blood spots on filter papers must be examined to prove that they truly reflect the data obtained from neonatal Guthrie cards. We should also examine whether screening can reduce the cost of treatment of the bacterial infections and chronic lung diseases in patients with XLA and non-XLA and increase the benefits for these patients. An anticipated pilot study using a large cohort of newborns must address these problems. We also found that T-cell–receptor excision circles and sjKRECs can be measured simultaneously on the same plate. Thus, a pilot study of neonatal screening for both T-cell and B-cell deficiencies could be performed simultaneously.

We thank the patients and their families who participated in this study. We also thank Ms Makiko Tanaka and Ms Kimiko Gasa for their skillful technical assistance and members of the Department of Obstetrics and Gynecology at the National Defense Medical College for collecting umbilical cord blood samples as well as Drs Wataru and Masuko Hirose. We are also indebted to Prof J. Patrick Barron, Chairman of the Department of International Medical Communications of Tokyo Medical University, for his *pro bono* linguistic review of this article.

Noriko Nakagawa, MD[a]
Kohsuke Imai, MD, PhD[a,b]
Hirokazu Kanegane, MD, PhD[c]
Hiroki Sato, MS[b]
Masafumi Yamada, MD, PhD[d]
Kensuke Kondoh, MD, PhD[e]
Satoshi Okada, MD, PhD[f]
Masao Kobayashi, MD, PhD[f]
Kazunaga Agematsu, MD, PhD[g]
Hidetoshi Takada, MD, PhD[h]
Noriko Mitsuiki, MD[i,j]
Koichi Oshima, MD[j,k]
Osamu Ohara, PhD[j]
Deepti Suri, MD[l]
Amit Rawat, MD[l]
Surjit Singh, MD[l]
Qiang Pan-Hammarström, MD, PhD[m]
Lennart Hammarström, MD, PhD[m]
Janine Reichenbach, MD[n]
Reinhard Seger, MD[n]
Tadashi Ariga, MD, PhD[d]
Toshiro Hara, MD, PhD[h]
Toshio Miyawaki, MD, PhD[c]
Shigeaki Nonoyama, MD, PhD[a]

From [a]the Department of Pediatrics, National Defense Medical College, and [b]the Department of Medical Informatics, National Defense Medical College Hospital, Saitama, Japan; [c]the Department of Pediatrics, University of Toyama, Toyama, Japan; [d]the Department of Pediatrics, Hokkaido University, Hokkaido, Japan; [e]the Department of Pediatrics, St Marianna University School of Medicine, Kanagawa, Japan; [f]the Department of Pediatrics, Hiroshima University, Hiroshima, Japan; [g]the Department of Pediatrics, Shinshu University, Nagano, Japan; [h]the Department of Pediatrics, Kyushu University, Fukuoka, Japan; [i]the Department of Pediatrics, Tokyo Medical and Dental University, Tokyo, Japan; [j]the Department of Human Genome Technology, Kazusa DNA Research Institute, Chiba, Japan; [k]the Department of Clinical Application, Center for iPS Cell Research and Application, Kyoto University, Kyoto, Japan; [l]the Advanced Pediatric Centre Post Graduate Institute of Medical Education and Research, Chandigarh, India; [m]the Division of Clinical Immunology, Department of Laboratory Medicine, Huddinge Hospital, Karolinska Institute, Stockholm, Sweden; and [n]the Department of Immunology/Hematology/BMT, University Children's Hospital Zurich, Zurich, Switzerland. E-mail: kimai@ndmc.ac.jp.

Supported in part by grants from the Ministry of Defense; the Ministry of Health, Labor, and Welfare; the Ministry of Education, Culture, Sports, Science and Technology; and the Kawano Masanori Foundation for Promotion of Pediatrics.

Disclosure of potential conflict of interest: The authors have declared that they have no conflict of interest.

REFERENCES

1. Conley ME, Broides A, Hernandez-Trujillo V, Howard V, Kanegane H, Miyawaki T, et al. Genetic analysis of patients with defects in early B-cell development. Immunol Rev 2005;203:216-34.
2. Kanegane H, Futatani T, Wang Y, Nomura K, Shinozaki K, Matsukura H, et al. Clinical and mutational characteristics of X-linked agammaglobulinemia and its carrier identified by flow cytometric assessment combined with genetic analysis. J Allergy Clin Immunol 2001;108:1012-20.
3. Plebani A, Soresina A, Rondelli R, Amato GM, Azzari C, Cardinale F, et al. Clinical, immunological, and molecular analysis in a large cohort of patients with X-linked agammaglobulinemia: an Italian multicenter study. Clin Immunol 2002;104:221-30.
4. Siminovitch KA, Bakhshi A, Goldman P, Korsmeyer SJ. A uniform deleting element mediates the loss of kappa genes in human B cells. Nature 1985;316:260-2.
5. van Zelm MC, Szczepanski T, van der Burg M, van Dongen JJ. Replication history of B lymphocytes reveals homeostatic proliferation and extensive antigen-induced B cell expansion. J Exp Med 2007;204:645-55.
6. Eades-Perner AM, Gathmann B, Knerr V, Guzman D, Veit D, Kindle G, et al. ESID Registry Working Party. The European internet-based patient and research database for primary immunodeficiencies: results 2004-06. Clin Exp Immunol 2007;147:306-12.
7. Morinishi Y, Imai K, Nakagawa N, Sato H, Horiuchi K, Ohtsuka Y, et al. Identification of severe combined immunodeficiency by T-cell receptor excision circles quantification using neonatal Guthrie cards. J Pediatr 2009;155:829-33.
8. Ozyurek E, Cetintas S, Ceylan T, Ogus E, Haberal A, Gurakan B, et al. Complete blood count parameters for healthy, small-for-gestational-age, full-term newborns. Clin Lab Haematol 2006;28:97-104.
9. Comans-Bitter WM, de Groot R, van den Beemd R, Neijens HJ, Hop WC, Groeneveld K, et al. Immunophenotyping of blood lymphocytes in childhood: reference values for lymphocyte subpopulations. J Pediatr 1997;130:388-93.
10. Kaneko H, Kawamoto N, Asano T, Mabuchi Y, Horikoshi H, Teramoto T, et al. Leaky phenotype of X-linked agammaglobulinaemia in a Japanese family. Clin Exp Immunol 2005;140:520-3.

Available online March 11, 2011.
doi:10.1016/j.jaci.2011.01.052

TABLE E1. Characteristics of patients with XLA

Patient no.	Unique patient no.	Age (y)	Sex	Serum Ig (mg/dL)			$CD19^+$		*BTK* mutation			Source	
				IgG	IgA	IgM	% Lymph	/μL	Genomic DNA	cDNA	Amino acid	Guthrie	Dry spot
P1	670	0	M	87	<6	10	0.21	12.99	29269G>T	1178-1G>T	Splice acceptor defect	x	
P2	718	0	M	215	<10	<10	0.07	7.04	11593_11594 insA	144_145insA	Arg49 frameshift	x	
P3	722	0	M	80	<1	1	<1.00	NA	25644C>T	763C>T	Arg255X	x	
P4	727	8	M	295	59	57	0.11	3.52	29269G>T	1178-1G>T	Splice acceptor defect		x
P5	732	34	M	1140*	<6	8	0.02	0.24	11631T>A	182T>A	Ile61Asn		x
P6	811	24	M	458*	0	13	0.50	5.32	23570T>G	426T>G	Tyr142X		x
P7	813	18	M	628*	109	6	0.60	6.87	23570T>G	426T>G	Tyr142X		x
P8	814	19	M	260	0	NA	0.20	3.01	16180C>T	344C>T	Ser115Phe		x
P9	815	13	M	600*	<10	<5	0.08	1.72	11590G>T	142-1G>T	Splice acceptor defect		x
P10	816	11	M	12	0	5	0.00	0.00	150kb deletion of *BTK, TIMM8A, TAF7L, DRP2*				x
P11	817	10	M	10	2	24	0.80	35.78	36288C>T	1928C>T	Thr643Ile		x
P12	824	13	M	462	6	27	0.41	14.49	27518C>A	895-11C>A	Splice acceptor defect		x
P13	834	5	M	<237	<37	43	0.00	0.00	25715_26210del	776+57_839+73del	Exon 9 deletion		x
P14	838	21	M	<50	<5	7	0.00	0.00	31596G>C	1631+1G>C	Splice donor defect		x
P15	839	16	M	604*	<1	<2	0.04	0.66	31596G>C	1631+1G>C	Splice donor defect		x
P16	847	11	M	698*	26	11	0.08	1.86	25536delG	655delG	Val219 frameshift		x
P17	877	14	M	20	19	8	0.21	NA	32357T>C	1750+2T>C	Splice donor defect		x
P18	880	5	M	233	39	41	0.06	NA	10941-?_14592+?del	1-?_240+?del	Exon 1-3 deletion		x
P19	888	8	M	<212	<37	150	0.15	6.60	11023G>A	83G>A	Arg28His		x
P20	891	21	M	195	<6	37	0.02	0.09	32243C>G	1638C>G	Cys502Trp		x
P21	958	0	M	<50	<10	9	0.80	27.14	31544_31547 delGTTT	1580_1583del GTTT	Cys527 frameshift		x
P22	701	2	M	115	<2	4	0.09	1.99	16172C>A	336C>A	Tyr112X		x
P23	911	0	M	<10	<6	<4	0.00	0.00	29955A>C	1350-2A>C	Splice acceptor defect	x	
P24	937	0	M	60	<2	58	0.00	0.00	11022C>T	82C>T	Arg28Cys	x	
P25	938	0	M	<20	<4	<6	0.00	0.00	36269-?_36778+?del	1909-?_2418+?del	Exon 19 deletion	x	
P26	939	0	M	60	<2	22	0.00	0.00	11022C>T	82C>T	Arg28Cys	x	
P27	890	12	M	<237	<37	<20	0.03	NA	36261G>A	1909-8G>A	Splice acceptor defect		x
P28	944	6	M	12	<1	1	0.02	NA	36281C>T	1921C>T	Arg641Cys		x
P29	948	5	M	<237	<37	<20	0.01	0.70	36261G>A	1909-8G>A	Splice acceptor defect		x
P30	1053	5	M	386	5	113	1.10	34.22	32259A>C	1654A>C	Thr552Pro		x

Age, Age at analysis of KRECs; *$CD19^+$ % Lymph,* CD19-positive cell percentage in lymphocytes; *$CD19^+$ /μL,* CD19-positive cell number in 1 μL whole peripheral blood; *M,* male; *NA,* not available; *Serum Ig,* serum levels of immunoglobulins at diagnosis.

BTK mutation's reference sequences are NCBI NC_000023.9, NM_000061.2, and NP_000052.1.

*Trough level during intravenous immunoglobulin therapy.

TABLE E2. Characteristics of patients with non-XLA

				Serum Ig (mg/dL)			$CD19^+$			Source	
Patient no.	Unique patient no.	Age (y)	Sex	IgG	IgA	IgM	% Lymph	/μL	*BTK* mutation	Guthrie	Dry spot
P31	596	4	F	386	<6	6	0.42	21.27	Normal		x
P32	719	0	F	<50	<5	<5	0.00	0.00	Normal	x	
P33	835	8	M	311	323	20	0.09	1.88	Normal		x
P34	915	0	M	<212	<37	<20	0.00	0.00	Normal		x
P35	947	0	M	<21	<37	<39	0.00	0.00	Normal		x

Age, Age at analysis of KRECs; *$CD19^+$ % Lymph,* CD19-positive cell percentage in lymphocytes; *$CD19^+$ /μL,* CD19-positive cell number in 1 μL whole peripheral blood; *F,* female; *M,* male; *Serum Ig,* serum levels of immunoglobulins at diagnosis.

J Clin Immunol (2011) 31:309–314
DOI 10.1007/s10875-010-9498-y

Clinical and Host Genetic Characteristics of Mendelian Susceptibility to Mycobacterial Diseases in Japan

Takayuki Hoshina · Hidetoshi Takada · Yuka Sasaki-Mihara · Koichi Kusuhara · Koichi Ohshima · Satoshi Okada · Masao Kobayashi · Osamu Ohara · Toshiro Hara

Received: 5 October 2010 / Accepted: 9 December 2010 / Published online: 8 January 2011

Abstract
Purpose The aim of this study is to investigate clinical characteristics and genetic backgrounds of Mendelian susceptibility to mycobacterial diseases (MSMD) in Japan.
Methods Forty-six patients diagnosed as having MSMD were enrolled in this study. All patients were analyzed for the *IFNGR1*, *IFNGR2*, *IL12B*, *IL12RB1*, *STAT1*, and *NEMO* gene mutations known to be associated with MSMD.
Results Six patients and one patient were diagnosed as having partial interferon-γ receptor 1 deficiency and nuclear factor-κB-essential modulator deficiency, respectively. Six of the seven patients had recurrent disseminated mycobacterial infections, while 93% of the patients without these mutations had only one episode of infection.
Conclusions The patients with a genetic mutation were more susceptible to developing recurrent disseminated mycobacterial infections. Recurrent disseminated mycobacterial infections occurred in a small number of patients even without these mutations, suggesting the presence of as yet undetermined genetic factors underlying the development and progression of this disease.

Keywords Disseminated mycobacterial infection · IFN-γR1 deficiency · NEMO deficiency · flow cytometric analysis

T. Hoshina · H. Takada (✉) · Y. Sasaki-Mihara · K. Kusuhara · T. Hara
Department of Pediatrics, Graduate School of Medical Sciences, Kyushu University,
3-1-1 Maidashi, Higashi-ku,
Fukuoka 812-8582, Japan
e-mail: takadah@pediatr.med.kyushu-u.ac.jp

K. Ohshima · O. Ohara
Laboratory for Immunogenomics,
RIKEN Research Center for Allergy and Immunology,
Yokohama, Japan

K. Ohshima · O. Ohara
Department of Human Genome Technology,
Kazusa DNA Research Institute,
Chiba, Japan

K. Kusuhara
Department of Pediatrics,
University of Occupational and Environmental Health,
Fukouka, Japan

S. Okada · M. Kobayashi
Department of Pediatrics, Hiroshima University
Graduate School of Biomedical Sciences,
Hiroshima, Japan

Introduction

Although the outcome of mycobacterial infection is influenced by many factors, including the virulence of the pathogen and the environment of the host, it has been demonstrated that host genetic factors play important roles in the defense against mycobacteria [1]. Mendelian susceptibility to mycobacterial diseases (MSMD, MIM 209950) is a rare primary immunodeficiency syndrome characterized by a predisposition to develop infections caused by weakly virulent mycobacteria, such as *Mycobacterium bovis* bacille Calmette-Guerin (BCG) and environmental non-tuberculous mycobacteria (NTM) [2–4]. These patients are vulnerable to systemic salmonellosis and infections with *Mycobacterium tuberculosis*, the virulent mycobacterial species, to a lesser extent [5, 6]. Diseases caused by other intracellular pathogens, such as *Nocardia*, *Listeria*, *Paracoccidioides*, *Histoplasma*, and *Leishmania*, and some viruses, such as human herpes virus-8, have only rarely been reported, mostly in single patients [7–12].